Russian Chemical Reviews **72** (3) 233 – 255 (2003) © 2003 Russian Academy of Sciences and Turpion Ltd

DOI 10.1070/RC2003v072n03ABEH000777

Modern applications of matrix isolation technique to investigation of radical species generated in atom – molecular chemical reactions

E Ya Misochko, A V Akimov, I U Goldshleger

Contents

I.	Introduction	233
II.	Low-temperature spectroscopy of matrix-isolated species as a tool for investigations of reactive intermediates	235
III.	Translational mobility of hydrogen, fluorine and oxygen atoms in the crystals and solid matrices of inert gases	240
IV.	Chemical reactions involving hydrogen atoms	241
V.	Chemical reactions involving fluorine atoms	244
VI.	Chemical reactions involving oxygen atoms	250
VII.	Conclusion	252

Abstract. The potential of using the translational mobility of hydrogen, oxygen and fluorine atoms in the crystals and solid matrices of inert gases for initiating solid-phase cryochemical reactions and for investigating the stabilised intermediate particles generated in these reactions is discussed. The main spectroscopic methods used to study the stabilised particles are considered. Particular emphasis is placed on elucidation of the spectroscopic characteristics required for reliable identification and determination of the structure of new reactive intermediates. Methodological approaches to the solution of this problem are discussed. Examples of successful implementation of these approaches by various research groups are given. The bibliography includes 205 references.

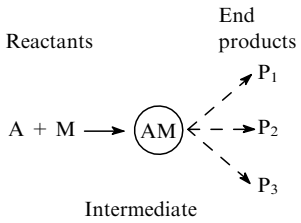
I. Introduction

Atom – molecular chemical reactions play an important role in various chemical and biological processes. Therefore, considerable attention has been given to applied studies of and basic research into such reactions. Experimental determination of the rate constants for most of the practically important atom – molecular reactions in the gas phase dates back to the latter half of the 20th century. However, the mechanisms of cleavage and formation of new chemical bonds in this type of reactions cannot always be described at the molecular level due to the lack of information on the dynamics of the reacting systems in the vicinity of the transition state.

A particular avenue of research in the field of modern chemical physics is the investigation of the dynamics of atom – molecular chemical reactions in which the formation of end products is preceded by binding the reactants into a long-lived (compared to the period of intramolecular vibrations) intermediate complex.

E Ya Misochko, A V Akimov, I U Goldshleger Institute of Problems of Chemical Physics, Russian Academy of Sciences, 142432 Chernogolovka, Moscow Region, Russian Federation. Fax (7-096) 524 96 76.
Tel. (7-096) 720 49 59 (ext. 2-1404).
E-mail: misochko@icp.ac.ru (E Ya Misochko), shura@icp.ac.ru (A V Akimov), ilya@icp.ac.ru (I U Goldshleger)

Received 10 October 2002
Uspekhi Khimii **72** (3) 262 – 286 (2003); translated by A M Raevsky



Of particular interest are the investigations of intermediate species (radical intermediates) involved in these reactions. This is due to a noticeable and sometimes even determining effect of these species on the ratio of the reaction products and on the energy distribution over their internal degrees of freedom. Experimental kinetic data as well as quantum-chemical calculations on this type of reactions in the gas phase indicate the possibility for a variety of reactive intermediates to exist. Nevertheless, spectroscopic information on the intermediate species of most of the reactions in question is unavailable as yet. Detection of such intermediates in the gas phase is a rather complicated problem since the intermediate products usually have short lifetimes because of high collision energies of reactants in the reactions occurring under normal conditions.

Traditionally, information on the reaction dynamics of elementary processes in the gas phase has been obtained using the molecular beam technique which allows measurements of the energy and angular distributions of products formed in the atom + molecule collision reactions. However, these experiments provide indirect information on the reactive intermediates, since the behaviour of the reacting system in the vicinity of the transition state is reconstructed from the data on the state of the end reaction products. Improved experimental techniques combining supersonic cooling of gas jets and spectroscopic methods with high temporal resolution [1, 2] are based on the concept of studying the chemical dynamics of a system with a temporal resolution that is better (shorter) than the characteristic times of intramolecular motions. This permits obtaining information on the potential energy surface (PES) of reactions in the vicinity of the transition state. However, these methods are applicable to a narrow range of objects due to the requirement of high sensitivity and temporal resolution imposed on the measurements carried out under conditions when the system is 'frozen' in configuration on the femtosecond time scale.

Another approach to the investigation of short-lived intermediates in the gas phase involves freezing of reactive intermedi-

ates at cryogenic temperatures. In the simplest version of this technique products of a gas-phase reaction are trapped and frozen in a matrix consisting of a large excess of inert gas. The use of inert gases as solid matrices for spectroscopic investigations of radical species was proposed in the studies of research groups headed by Pimentel and Porter in 1954.[3,4] These studies marked the beginning of intensive development of the matrix isolation technique. The vast majority of species trapped in the matrices of inert gases exhibit no translational mobility at temperatures up to the melting (sublimation) temperature of the crystal of inert gas. This allows accumulation of sufficiently high concentrations of radicals and their detection by continuous-wave spectroscopic techniques. It is these methods that were employed to obtain spectroscopic data for most of the known free radicals; this information is generalised and systematised on a regular basis.[5] An essential drawback of the technique is the interaction between the species under study and the crystalline environment, which inevitably causes changes in their spectroscopic characteristics. Therefore, molecular beam spectroscopy provides more accurate information on subtle features of the molecular structure and properties of reactive intermediates. Nevertheless, versatility and the possibility of using continuous-wave spectroscopic equipment for detecting new molecules and obtaining primary characteristics of their structures make the matrix isolation technique a basic experimental method of research in such fields of science as chemical physics and molecular spectroscopy.

During the last 50 years the concept of matrix isolation of radical species developed in two main directions, namely, search for new conditions for generation of reactive intermediates and the use of various spectroscopic methods for their studies. These research avenues have been reviewed.[6–8] In the mid-1960s, Milligan and Jacox proposed [9] that, would the atoms of light elements (*e.g.*, hydrogen) have sufficiently high translational mobility in low-temperature matrices, the reactive intermediates could be stabilised by generating them *in situ* in the reactions of the mobile atoms with molecules of the other reactant trapped in the inert matrices.

Indeed, at ultralow temperatures ($\leqslant 50$ K) the solid matrix acts as an inert chemical microreactor which permits fast relaxation of the excess energy of the reaction and prevents the reaction products from flying apart. The matrix also provides ideal conditions for stabilisation of the reactive intermediates characterised by short lifetimes in the gas phase. To illustrate their hypothesis, Milligan and Jacox carried out spectroscopic studies of the products of photolysis of HI molecules in dilute $Ar/HI/O_2$ solid mixtures and first determined the vibrational frequencies of the $HO_2^{\bullet}$ radical. They assumed that this radical is produced in the reaction of the migrating photogenerated hydrogen atom with oxygen molecule trapped in the inert matrix,

$$H + O_2 \longrightarrow HO_2^{\bullet}. \qquad (1)$$

Obtaining new experimental data on the mobility of various atoms in cryogenic crystals and solid matrices in the last decade gave an impetus to further development of this concept. Since the early 1990s a large number of studies on the conditions for generation of atoms in solid matrices by photolysis of trapped molecules have been reported. It was established that in some cases the 'cage effect', which precludes photodissociation of molecules in solids, is insignificant and generation of atoms in inert matrices can occur with quantum yields close to unity. A large number of studies provide only qualitative data which permits ambiguous interpretation from the standpoint of physical mechanisms. Nevertheless, they point to the possibility for particular atoms to migrate over rather long distances in the crystals and matrices of inert gases. The results obtained were generalised in a review [10] which also concerns possible mechanisms of translational mobility of atoms at ultralow temperatures, namely, migration and thermalisation of a translationally excited 'hot' atom generated upon photodissociation of precursor molecule as well as thermal and photostimulated diffusion of atoms.

In this review we discuss the potentialities of using mobile atoms in cryogenic solid matrices for generation and investigation of reactive intermediates. The data on the mobility of various atoms are presented, methodological approaches aimed at solving the problem posed are outlined and some examples of their practical implementation are given.

We will consider reactions with participation of reactive atoms of only three elements, that is, hydrogen, fluorine and oxygen, involved in various practically important processes. The relatively simple electronic structure of these atoms facilitates analysis of the various elementary processes they are involved in. Two different [from the standpoint of their chemical reactions in solid matrices (crystals) of inert gases] types of mobile atoms considered in this review are translationally excited 'hot' atoms and diffusing thermalised atoms.

To generate reactive intermediates in a solid-phase chemical reaction in crystals at ultralow temperatures, the following conditions should be met:

— the molecules of reactant and photolytic precursor of atoms must be initially isolated in the sample;

— the atom must be mobile to migrate in the solid matrix;

— the energy of the atom must be high enough to overcome the barrier to reaction.

This shows the interrelation between matrix isolation techniques and preparative-scale cryochemistry. They have much in common from the standpoint of methodology but are mutually excluding in their basic formulations, namely, matrix isolation implies the absence of chemical transformations while the subject of cryochemistry is specific features of chemical reactions at ultralow temperatures.[11,12]

In this review cryochemical reactions of mobile atoms are treated as a means of generation of reactive intermediates while spectroscopic methods of investigation are considered as experimental techniques for studying matrix-isolated particles. This concept predetermines the issues that have attracted primary attention in this review. First of all, investigations of chemical transformations require relevant kinetic measurements to establish the principal reaction channels in the reacting system and to identify the primary and subsequent reactions. Carrying out spectroscopic measurements, one should choose spectroscopic characteristics necessary for reliable identification of particles. This is of particular importance in studies of novel open-shell species that were not observed earlier by other experimental methods.

Isotope substitution has been traditionally employed in analysis of vibrational and EPR spectra. Until recently, in most cases analysis of the spectra of isotopomers with the same stoichiometry served as the only objective argument when identifying new stabilised particles and establishing their structure. Improvement of computer hardware and development of new methods of quantum-chemical calculations in the last 10–15 years brought about radical changes in the procedure for identification and characterisation of trapped intermediates. Experimental data on the structure of most reactive intermediates are scarce, which precludes evaluation of the reliability and accuracy of calculations. It should be noted that quantum-chemical calculations should be treated as a kind of prediction until confirmation by corresponding experimental data. However, the use of modern methods of quantum-chemical calculations permits reliable identification of new chemical compounds based on comparison of the calculated and experimental spectroscopic data. In this review particular emphasis has been placed on joint use of experimental (both spectroscopic and kinetic) data and the results of quantum-chemical calculations of reactive intermediates.

II. Low-temperature spectroscopy of matrix-isolated species as a tool for investigations of reactive intermediates

1. Vibrational spectroscopy

The absorption IR spectroscopy is the most widely used method of investigation of matrix-isolated particles. Using this technique implies that the interaction of impurity particles with the lattice of inert gas is weak and has only little effect on the structure and vibrational dynamics of the species under study. The relative matrix shifts of vibrational frequencies (ratio of the frequency difference between the molecular vibration in the solid matrix and in the gas phase to the vibrational frequency in the gas phase) of various molecules and radicals have been analysed.[13] For most molecules the matrix shifts were found to lie between -2% and 2% (Fig. 1). The matrix shift histogram presented is centred at $\sim 0.5\%$ while the dispersion is at most 1%. The magnitude and sign of the matrix shift are related to the character of intermolecular interactions between the particle and environment. In some cases one should take into account the dynamic effects in addition to static guest – host interactions. Modern computational approaches to determination of matrix shifts have been documented.[14, 15]

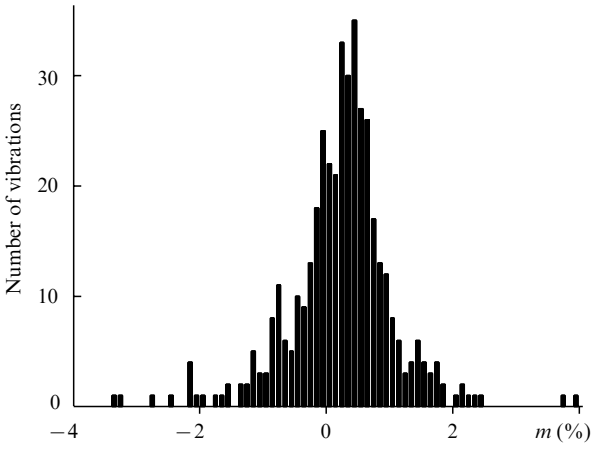


Figure 1. Relative matrix shifts (m) of vibrational frequencies of intermediates isolated in argon matrices.[13]

Head-Gordon *et al.*[16] reported comparative analysis of the accuracy of calculations of vibrational frequencies for various molecular compounds using the most widely used *ab initio* computational methods (in the harmonic approximation). The accuracy of B3LYP density functional calculations of fundamental frequencies was shown to be comparable with that of the frequency calculations by the CCSD(T) method. For instance, the frequencies obtained from B3LYP/cc-pVDZ calculations deviate from the corresponding frequencies measured in the gas phase by $\sim 5\%$ on the average, while the relative error of CCSD(T)/cc-pVDZ calculations can be as high as 1.5%. At the same time, all computational methods employed give a rather wide scatter of deviation values (dispersion of the deviations from the experimental values amounts to 10% – 12%). The most complicated problems are associated with calculations of the vibrational frequencies of light atoms (in particular, hydrogen atom) in polyatomic molecules.

The potentialities of IR spectroscopy are extended with improvement of corresponding equipment. Currently, the technique permits reliable detection of molecular compounds under study at concentrations that are low enough to provide conditions for spatial isolation of these species in a solid matrix. A conventional procedure for preparation of solid samples of an inert gas, containing trapped impurity molecules, involves condensation of the gas molecular beams *in vacuo* on a substrate cooled to helium temperatures. Thin films of inert gas thus obtained have a polycrystal morphology and are characterised by the presence of nonequilibrium defects and a large specific surface. Usually, such films are called 'solid matrices'; however, one should keep in mind a basic difference between these films and crystals grown under equilibrium conditions. It is nonequilibrium conditions for condensation and low concentrations of impurity particles that allow trapping of virtually any particle in the matrix without their association. Long-range order in the vicinity of the small impurity molecules trapped in a solid matrix corresponds, as a rule, to substitutional impurity or to interstitial impurity occupying the O_h site in the face-centred cubic (f.c.c.) lattice of inert gas.[14] An impurity trapped in a solid matrix is considered isolated if its nearest environment contains no analogous particle. If the trapped molecules are randomly distributed over the substitutional sites of a f.c.c. crystal lattice, the probability, p, for a particular molecule to be spatially isolated is given by the following expression,

$$p \approx 1 - z x_m ,$$

where $z = 12$ is the number of atoms in the first coordination sphere of the impurity molecule and x_m is the relative concentration of impurity particles (x_m = [m]/[Ar]). To consider a total of 99% of impurity particles isolated, their concentration x_m should be less than 10^{-3}. In real experiments the number of trapped dimers and higher clusters of impurity molecules much exceeds the statistical average. This is usually explained by limited mobility of the molecules on the surface of the growing film during condensation and by their interaction in the gas mixture. If only van der Waals intermolecular interactions occur, the fraction of clusters amounts, as a rule, to 1% – 5% of the total number of trapped molecules at $x_m \simeq 5 \times 10^{-4}$. If the molecules are capable of forming hydrogen-bonded clusters (*e.g.*, NH_3 and HCN, see Refs 17 – 19), this proportion increases to 10% – 20%.

The sensitivity of IR spectroscopic measurements in the conventional spectral range (400 – 4000 cm^{-1}) under conditions of matrix isolation of the particles under study can be estimated based on the characteristic values of the integrated intensity ($B \approx 10^7$ cm mol^{-1}) and spectral halfwidth ($\Delta \approx 3$ cm^{-1}) of absorption bands. At optical densities $D > 2 \times 10^{-3}$, these values correspond to a measurable number of particles, $N > 5 \times 10^{14}$ cm^{-2}. In this case, assuming that the thickness of the matrix film is ~ 100 μm, the average relative concentration of the particles to be recorded is greater than 10^{-6}. These values allow measurements of the IR spectra using low concentrations (sufficient for spatial isolation) of reactant molecules. Usually, the relative concentrations of impurity molecules are of the order of $10^{-3} - 10^{-4}$. This permits both reliable detection of weak bands in the IR spectrum (with the integrated absorption coefficient of about $10^5 - 10^6$ cm mol^{-1}) and measurements of changes in the concentrations of initial reactants in the course of chemical transformations with an error of at most 0.5%.

IR spectroscopy allows detection of different types of particles (molecules, radicals, ions, molecular complexes). Therefore, this method is a universal tool for kinetic measurements. The potential of the technique, as applied to differentiation between particular bands in the IR spectrum of products of the reactions of mobile atoms based on the results of kinetic measurements, was demonstrated taking reactions of fluorine atoms with CO molecules in solid argon at 20 K as examples.[20, 21] In this case, where only one reactant (fluorine atom) is mobile in the matrix, the principal channels of consumption of the reactants are as follows:
recombination of diffusing fluorine atoms

$$F + F \longrightarrow F_2 , \qquad (2a)$$

primary reaction of fluorine atoms

$$F + CO \longrightarrow FCO^{\bullet} , \qquad (2b)$$

secondary reaction of fluorine atoms

$$F + FCO^{\bullet} \longrightarrow F_2CO. \quad (2c)$$

The experimentally observed changes in the band intensities in the IR spectrum of the reactant molecule (CO) and reaction products correspond to this simple kinetic scheme. Namely, in the initial stage, the intensities of the bands of the molecular product (F_2CO) increase quadratically with respect to the increase in the intensities of the bands of $FCO^{\bullet}$ radicals and those of the consumption of the molecular reactant. This allows one to distinguish between the IR bands of the primary and secondary products of the reactions of the mobile atoms. One can also measure the absolute intensities of the bands by comparing the increase in the band intensity and the corresponding decrease in the intensities of the bands of the reactant molecules. Taking into account the mass balance equation for the CO group,

$$\Delta[CO] = \Delta[FCO^{\bullet}] + \Delta[F_2CO] \quad (3)$$

one gets a linear relation between the product band intensities, $A_{FCO^{\bullet}}$ and A_{F_2CO}, normalised to the corresponding decrease in the intensity of the band of the molecular reactant, ΔA_{CO}

$$\frac{A_{FCO^{\bullet}}}{\Delta A_{CO}} = -\beta_1 \frac{A_{F_2CO}}{\Delta A_{CO}} + \beta_2, \quad (4)$$

where β_1 and β_2 are the ratios of the integrated intensities of the bands

$$\beta_1 = \frac{B_{FCO^{\bullet}}}{B_{F_2CO}}, \ \beta_2 = \frac{B_{FCO^{\bullet}}}{B_{CO}}. \quad (5)$$

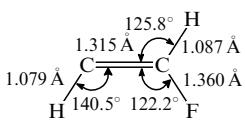
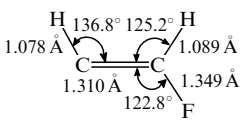
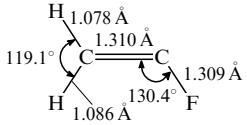
Since the ratio of the concentrations of the primary and secondary reaction products varies in the course of transformations, the relative absorption coefficients for the products and reactant, $B_{FCO^{\bullet}}/B_{CO}$ and B_{F_2CO}/B_{CO}, can be determined from the linear dependence of the relative intensities of the product bands in Eqn (4). Experiments showed [20] that the band intensities of the molecular product (F_2CO) thus obtained are in agreement with those determined earlier by other methods and that the band intensities of the radical product ($FCO^{\bullet}$) are in reasonable agreement with the results of corresponding quantum-chemical calculations.

Despite high sensitivity and versatility of IR spectroscopy, identification of radical intermediates and determination of their structure faces some problems. For instance, if we deal with condensation of reaction products from the gas phase, the IR bands of different products cannot always be reliably distinguished and identified. As mentioned above, carrying out solid-phase reactions eliminates this problem. Another type of severe problem is associated with the fact that the vibrational frequencies measured by IR spectroscopy are dynamic characteristics of molecular compounds. Therefore, in some cases determination of the molecular structure based on the vibrational spectra only is complicated and additional information is required. This is of particular importance in studies of loosely bound molecular complexes or various isomers and conformers of trapped intermediates. Registration of characteristic low-frequency vibrations ($\nu \leqslant 300\ cm^{-1}$) of loosely bound complexes using conventional instruments is also difficult. Moreover, both static deformations of the structure and dynamic lattice effects predetermine large shifts of the vibrational frequencies of complexes.

When studying various isomers of the same stoichiometry, one should take into account minor changes in the vibrational dynamics of different isomers, especially if changes in position of the hydrogen atom are concerned. In this case changes in the characteristic vibrational frequencies are comparable with the accuracy of calculations. Therefore, identification of a particular isomer of a stabilised radical by comparing the experimental and calculated vibrational spectra is complicated.

As an example, Table 1 lists the geometric parameters, vibrational frequencies and isotropic hyperfine coupling constants (IHFC) of structural isomers of the 2-$C_2H_2F^{\bullet}$ radical generated in the reaction of a mobile fluorine atom with a C_2H_2 molecule in

Table 1. Calculated and experimental vibrational frequencies and isotropic hyperfine coupling constants of structural isomers of 2-$C_2H_2F^{\bullet}$ radical. Calculations were carried out by the B3LYP/6-311 + + G(3df,2p) method.

Parameter (vibration)	Calculated value [a]			Experimental value [a]	Experiment value [b]
	trans-2-$C_2H_2F^{\bullet}$	*cis*-2-$C_2H_2F^{\bullet}$	1-$C_2H_2F^{\bullet}$		
					
Vibrational frequencies /cm^{-1}					
1a' (CH_α stretching)	3307	3308	3236	3193	3178
2a' (CH_β stretching)	3184	3122	3111	3026	–
3a' (CC stretching)	1664	1678	1701	1631	1623
4a' ($H_\beta CC$ bending)	1305	1291		1263	1211
(CH_2 bending)			1395		
5a' (CF stretching)	1024	1093	1149	1070	1066
6a' ($H_\alpha CC$ bending)	779	734		698	678
(CH_2 rock)			943		
7a' (FCC bending)	433	479	454	–	462
1a'' (wagging)	883	827	831	785	785
2a'' (twist vibrations)	661	645	615	643	631
IHFC constant /mT (see[c])					
a_F	10.12	6.69	13.37	|6.50|	|7.30|
a_{H_β}	1.69	3.81	4.16	|3.86|	|3.81|
a_{H_α}	0.14	0.17	1.20	|0.25|	–

[a] The data were taken from Ref. 22; the vibrational frequencies were calculated in the harmonic approximation. [b] The vibrational frequencies were taken from Ref. 23 and the IHFC constants were taken from Ref. 24. [c] Only absolute values of IHFC constants were measured experimentally.

solid argon [22] as well as the results of an earlier study [23] in which the 2-$C_2H_2F^{\bullet}$ radicals were stabilised by condensation of reaction products in gas discharge. Analysis of the vibrational dynamics in the model structure of the *trans*-2-$C_2H_2F^{\bullet}$ isomer suggested [23] that the radical stabilised corresponds to this isomer. However, as can be seen in Table 1, the vibrational frequencies of the *trans*-2-$C_2H_2F^{\bullet}$ and *cis*-2-$C_2H_2F^{\bullet}$ isomers calculated by modern quantum-chemical methods are close and the experimental IR spectra cannot be assigned to a particular isomer even taking into account the results of analogous measurements for the deuterated analogue (2-$C_2D_2F^{\bullet}$). Comparison of the spectra of the radicals [22, 23] reveals close values of all vibrational frequencies (to an accuracy of ± 15 cm^{-1}), except for the relatively weak bending vibration $H_\beta CC$, for which the frequency difference is 52 cm^{-1}. However, the reason for such a large difference is still to be clarified (this can be different matrix shifts due to a different manner of arrangement of the radical in the lattice, or these are different isomers, or incorrect assignment of the weak IR band!?). Moreover, identification of another structural isomer, 1-$C_2H_2F^{\bullet}$, faces analogous problems since the patterns of the vibrational spectra of all three particles are similar and exhibit no characteristic distinctive features (see Table 1). Unambiguous establishment of the structure of radical intermediates in the two above-mentioned cases can be made only by joint use of vibrational and EPR spectroscopy.[22, 25]

2. EPR spectroscopy

Electron paramagnetic resonance is widely used in various applications of the matrix isolation technique as well as in cryochemical and radiation chemistry studies. Some key aspects of the use of this method in studies of matrix-isolated reactive intermediates are considered below.

High spectral resolution and sensitivity of the EPR technique under conditions of generation of radical intermediates in solid-phase reactions of mobile atoms with isolated reactant molecules are due to the following factors: perfect isolation of the radicals stabilised and the absence of radical pairs in the nearest environment (this eliminates the dipole – dipole interaction between radicals), the absence of super-HFC on the matrix nuclei due to zero nuclear spins of argon and neon atoms (and the ^{4}He and parahydrogen molecules), and fast (incoherent) rotation of radicals in the lattice, which averages anisotropic magnetic interactions.

These factors are due to both the procedure for generation of radicals and the properties of the inert matrices. Under conditions of ideal matrix isolation of the radicals the widths of individual components of the hyperfine structure (HFS) are at most 0.1 mT in solid argon and at most 0.01 mT in solid p-H_2. Therefore, the spectral resolution under these conditions is no worse than in liquids [26] and much better than in organic crystals and glasses.[27] The spectroscopic parameters of ethyl radicals measured in different media are listed in Table 2. As can be seen, the intrinsic widths of the lines in the spectra of radicals stabilised in solid parahydrogen or argon is comparable with the linewidths in the EPR spectra recorded in the liquid phase.[28 – 33]

A feature of small polyatomic molecules is rotation in solid matrices and crystals at ultralow temperatures. Depending on the species size and on site occupied by the particles in the crystal lattice, both free rotation (with population of nonzero rotational quantum states) and rotational diffusion (incoherent rotation) characterised by the rotational correlation time, τ_c, can occur. Fast incoherent rotation of radicals in the lattice causes averaging of anisotropic interactions, thus providing high resolution of the hyperfine structure and the possibility of determining the absolute values of the IHFC constants if they exceed 0.1 mT.

As an example illustrating the influence of various factors on the resolution of the EPR spectra of trapped radicals, Fig. 2 presents the spectra of the 2-$C_2H_2F^{\bullet}$ radicals generated in the solid-phase reaction $F + C_2H_2$. Spectrum *1* was obtained in an argon matrix with high concentration of C_2H_2, while spectrum *2* was recorded in a krypton matrix containing magnetic nuclei (the nuclear spin of ^{83}Kr atom is 9/2). In the former case most of the reactant molecules (C_2H_2) exist as dimers and more complex associates. This leads to stabilisation of the radicals bound in complexes with the neighbouring C_2H_2 molecules. The radical – molecule interaction in these complexes stabilises the structure formed and hinders rotation of the radical. Probably, that is why no resolved hyperfine structure of these radicals in photolysed mixtures $Ar : F_2 : C_2H_2(C_2D_2) = 200 : 1 : 1$ was recorded earlier.[34] A hyperfine splitting of 0.25 mT on the α-proton of the 2-$C_2H_2F^{\bullet}$ radical was first observed under conditions of perfect isolation of the radicals generated in the reactions of

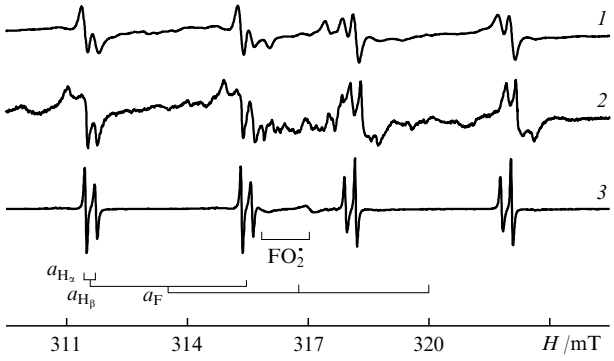


Figure 2. EPR spectra of 2-$C_2H_2F^{\bullet}$ radicals produced by photolysis at 15 K and subsequent annealing of the samples at 25 K.[22]
The spectra were recorded at 30 K; shown are the HFS of 2-$C_2H_2F^{\bullet}$ and $FO_2^{\bullet}$ radicals. Sample composition: $Ar : F_2 : C_2H_2 = 300 : 1 : 1$ (*1*), $Kr : F_2 : C_2H_2 = 3000 : 1 : 1$ (*2*) and $Ar : F_2 : C_2H_2 = 3000 : 1 : 1$ (*3*).

Table 2. Characteristic EPR linewidths, parameters of the hyperfine coupling (mT) and *g*-factor tensors of $C_2H_5^{\bullet}$ radical in different media.

Matrix	Generation technique	Linewidth	*g*-Factor	$\lvert a_\alpha \rvert$ [a]	$\lvert A_\perp^\alpha - A_\parallel^\alpha \rvert$	$\lvert a_\beta \rvert$	$\lvert A_\perp^\beta - A_\parallel^\beta \rvert$	Ref.
p-H_2 (>99.5%)	UV photolysis of C_2H_5I	0.02	2.0031 ($\Delta g \leqslant 0.0001$)	2.27	0.98	2.68	0.31	28
Ar	addition reaction $H + C_2H_4$	0.1	2.0023 ($\Delta g \leqslant 0.0003$)	2.28	1.02	2.68	0.28	29
C_2H_6 (liq.)	electron beam irradiation	0.01	2.0026	2.238	–	2.687	–	30
p-H_2 (>95%)	UV photolysis of C_2H_5I	0.14	–	2.24	–	2.69	–	31
Ar	the same	0.2	–	1.99	–	2.65	–	32
Xe	addition reaction $H + C_2H_4$	0.3	2.0026 ($\Delta g \leqslant 0.0015$)	2.25	0.93	2.72	0.36	33
Xe	abstraction reaction $H + C_2H_6$	0.3	2.0028 ($\Delta g \leqslant 0.0024$)	2.20	0.96	2.70	0.31	33

[a] Calculated using the formula $a = \dfrac{2A_\perp + A_\parallel}{3}$.

mobile atoms in solid argon (see spectrum *3* in Fig. 2). Experiments with heavier isotopomers of acetylene (C_2D_2 and C_2HD) allowed assignment of a complete set of IHFC constants of this type of radicals.[22] Analogously, frozen van der Waals complexes $FCO^{\bullet}\text{---}(CO)_n$ were produced in the samples with relative concentrations of the reactant molecules, $[CO] > 10^{-3}$ (see Refs 35 and 36). The EPR spectra of $FCO^{\bullet}$ radicals at 4.2 K provide a classical example of the EPR spectra of frozen radicals with strong anisotropy of the constants of HFC with the fluorine atom. Recently,[37] it was found that anisotropic spectra of the $FCO^{\bullet}$ radicals (they are similar to the spectra reported earlier[34,35]) in photolysed $Ar/F_2/CO$ samples with a high concentration of the molecular reactant ($[CO] > 5 \times 10^{-3}$) remain unchanged up to 30 K. However, the shape of the EPR spectra of $FCO^{\bullet}$ radicals in the samples with much lower concentration of the reactant molecules ($[CO] < 10^{-3}$) changes dramatically upon temperature variation.

The EPR spectrum of $FCO^{\bullet}$ radicals is presented in Figure 3. This is a superposition of an anisotropic spectrum, which varies only slightly with temperature, and a spectrum whose pattern closely resembles that of an isotropic spectrum. The linewidths in the latter spectrum drastically decrease as the temperature increases at $T > 13$ K. The samples with the relative concentration of the reactant molecules of less than 10^{-4} are characterised by a virtual absence of radicals exhibiting anisotropic spectra at high temperatures. The time τ_c of the isolated radicals, estimated from changes in the linewidths under conditions of fast incoherent rotation, is $\sim 10^{-9}$ s at 30 K. Averaging of the anisotropy due to fast rotation of radicals in inert matrices at ultralow temperatures was also pointed out in other studies (*e.g.*, Refs 38 and 39). These examples demonstrate that under perfect isolation conditions, the anisotropy of magnetic interactions of not only small radicals (*e.g.*, $FCO^{\bullet}$) but also larger structures, (*e.g.*, $C_2H_2F^{\bullet}$) is averaged due to fast rotation of the species in the lattice.

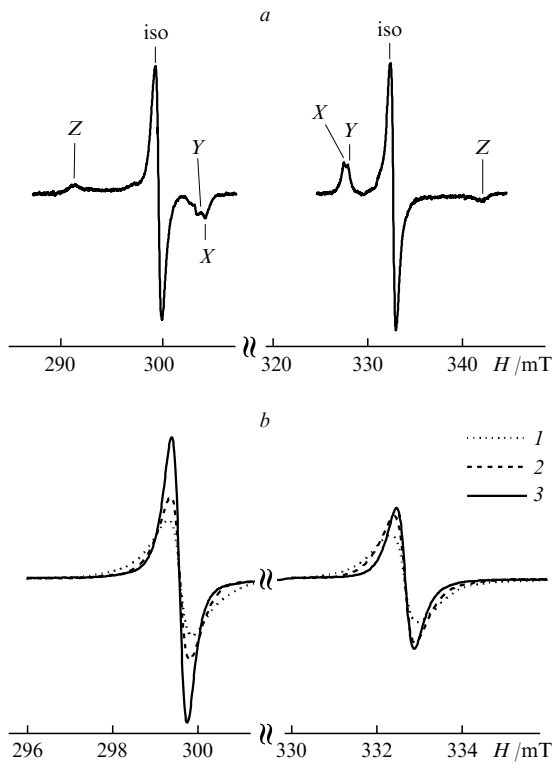


Figure 3. EPR spectra of $FCO^{\bullet}$ radicals in $Ar : F_2 : CO = 300 : 1 : 1$ (*a*) and $Ar : F_2 : CO = 3000 : 1 : 1$ (*b*) recorded at 15 (*1*), 22.5 (*2*) and 35 K (*3*).[37]
The components of the HFC tensor are labelled *X*, *Y* and *Z* and the isotropic line is labelled 'iso'.

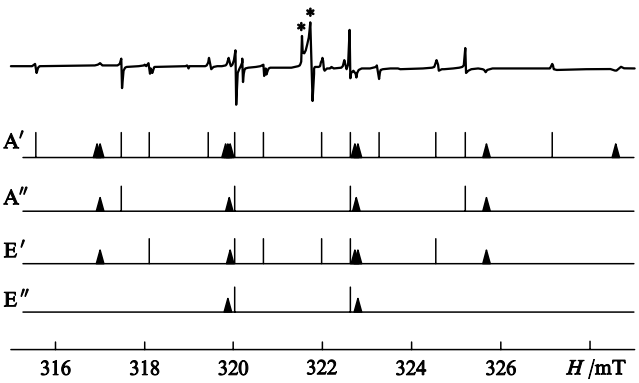


Figure 4. EPR spectrum of $p\text{-}H_2 : C_2H_5I = 5000 : 1$ sample after UV photolysis at 4.7 K.[28]
The intense signal at the centre of the spectrum (asterisked) is due to the presence of paramagnetic particles in the quartz ampoule. Shown are the calculated positions of the components of the anisotropic spectrum of ethyl radicals with A′, A″, E′ and E″ symmetry. Vertical lines and triangles denote positions of the components in the spectrum of ethyl radicals in which the C–C bond is respectively perpendicular and parallel to the direction of the external magnetic field.

Kumada *et al.*[28] reported the EPR spectra of $C_2H_5^{\bullet}$ radicals isolated in solid parahydrogen (Fig. 4). High spectral resolution achieved in this study (< 0.01 mT) allowed both determination of the anisotropic components of the HFC tensor in the absence of rotation of the whole radical and distinguishing between the spectral lines corresponding to different rotational states of the methyl group. The rotational energy level splitting in solid parahydrogen (5.3 ± 0.7 K) determined from temperature-induced variations of the line intensities was found to be close to that measured earlier by IR spectroscopy in the gas phase. Resolved EPR spectra of 2-fluoroethyl radicals can be recorded in solid argon under conditions of perfect isolation (Fig. 5).[40] Fast (incoherent) internal rotation and the dependence of the IHFC constants on the angle of rotation of the CH_2 group around the CH_2F fragment is responsible for a sharp temperature dependence of the EPR linewidths in the temperature range from 20 to 35 K. Anisotropy of the HFC tensor of the fluorine atom is retained upon warming up the system; therefore, changes in the spectral pattern are due to internal rotation of the CH_2 group only. Variation of the angle of rotation causes modulation of the HFC, thus leading to temperature-induced line broadening. The energy barrier, E_a, to internal rotation was estimated from the Arrhenius dependence of the linewidth at $\simeq 920 - 1050$ J mol^{-1},

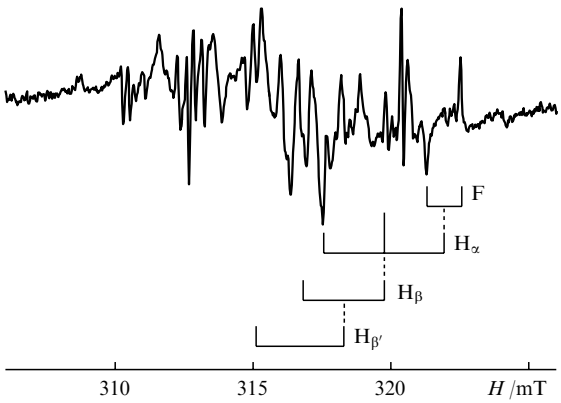


Figure 5. EPR spectrum of $2\text{-}C_2H_4F^{\bullet}$ radicals generated in reactions of diffusing fluorine atoms with C_2H_4 molecules and isolated in solid argon.[40]

which is close to the barrier height calculated [41] for a free radical in the gas phase. However, this value is much smaller than that measured in viscous liquids ($\sim$4000 J mol^{-1}).[42]

The aforesaid indicates that perfect isolation of radical species in inert matrices containing no magnetic nuclei permits both determination of the principal HFC parameters and characterisation of internal rotation of molecular fragments and atomic groups in the absence of rotation of the whole radical.

The experimentally measured IHFC constants provide a reliable structure-sensitive parameter suitable for identification of new radical intermediates. Their structures can be determined by comparing the experimental values of spectroscopic characteristics with the corresponding values calculated using modern quantum-chemical methods. This approach was substantiated [43–45] when analysing the experimental data and results of quantum-chemical calculations of different types of radicals. These investigations have demonstrated the practical applicability of density functional calculations to the studies of the interrelation between structure and spectroscopic characteristics. The IHFC constants are determined by the distribution of the unpaired electron density over the corresponding magnetic nuclei in the molecular structure. Therefore, these characteristics are rather sensitive to the changes in the electron wave function on the magnetic nuclei. The error in calculations of the IHFC constants using modern methods is usually at most 10%.[44] The vibrational frequencies can be calculated with better accuracy; however, they are much less sensitive to changes in the electronic structure. This is of crucial importance for the identification of reactive intermediates and for the determination of their structure in at least two critical situations. The first case concerns identification of a particular isomer of the stabilised intermediate. A typical example is provided by the *cis*- and *trans*-isomers of the 2-$C_2H_2F^{\bullet}$ radical. The vibrational spectra of these isomers were discussed above. As can be seen from Table 1, the values of the IHFC constants of the radicals stabilised in solid argon correspond to *cis*-2-$C_2H_2F^{\bullet}$ rather than *trans*-2-$C_2H_2F^{\bullet}$, as was reported earlier.[24,34] In this case both the chemical intuition (assignment of the experimental EPR spectrum was based on the assumption of analogy between the electron density distributions in the 2-$C_2H_2F^{\bullet}$ and $C_2H_3^{\bullet}$ radicals and on the predicted thermodynamic properties of the *cis*- and *trans*-isomers) and vibrational analysis [23] led to erroneous conclusions. This was first pointed out by Barone *et al*.[43] Reliable identification of the other structural conformer, 1-$C_2H_2F^{\bullet}$ radical, is possible only based on measurements of the IHFC constants. Insertion of a fluorine atom at the α-position causes a twofold increase in the IHFC constant a_F (and simultaneous increase in the IHFC constants on protons) compared to the corresponding constants of the isomers of the 2-$C_2H_2F^{\bullet}$ radical.

Another practically important problem is to determine the structure of weakly bound radical – molecular complexes. It has been shown [46,47] (for detailed analysis, see below) that reaction products of hydrogen abstraction from RH molecules can be stabilised in matrices in the form of radical – molecular complexes $R^{\bullet}$---HF. Taking into account the spectral resolution that can be achieved in the experiments with inert matrices, the EPR technique seems to be promising for the investigation of the structure of such intermediates. If the radical and the molecule in a complex are separated by at most 0.3 nm and the individual components of the HFS are no wider than 0.1 mT, the EPR spectra exhibit a resolved hyperfine structure corresponding to interactions of the unpaired electron of the radical with the magnetic nuclei of the other molecule (nuclear spin of the H and F atoms of the HF molecule is 1/2). The constants of magnetic interactions are rather sensitive to the distances and orientation of fragments in complexes; this permits their structure and sometimes the type and characteristic times of hindered internal motions of the fragments in the complex to be determined reliably.

3. Optical spectroscopy and photoinduced transformations of stabilised reactive intermediates

The main fields of application of the optical studies of cryogenic matrices involve spectroscopy of electronically excited states, photoinitiation of chemical transformations in the complexes comprised of molecular reactants, generation of radical species in the photodissociation of isolated molecules and photoinduced intramolecular conversion of isolated species as well as photostimulated translational mobility of atoms.

The electronic and vibronic transitions in the condensed phase are strongly affected by the environment, even if the molecular species under study are isolated in inert matrices. For this reason, spectroscopic investigations of matrix-isolated particles are to a greater extent focussed on the studies of the mechanisms of relaxation of excitation energy in the solid phase (see review [48]) rather than spectroscopic characterisation of excited states. Besides, instrumental problems due to strong scattering of the visible and UV light by crystalline matrix films, as well as the effects of nonradiative relaxation in the matrices reduce the sensitivity of absorption spectroscopy and limit the use of the laser-induced fluorescence (LIF) technique in these studies. Most spectroscopic data on the excited states of radical species were obtained in the gas-phase LIF and laser-induced magnetic resonance studies (these methods are characterised by high sensitivity and the possibility of carrying out experiments with spectral and temporal resolution). Detailed investigations of the $OH^{\bullet}$ (see Ref. 49), $CN^{\bullet}$ (see Refs 50 and 51) and $ClO_2^{\bullet}$ (see Refs 52–54) radicals were performed, and considerable attention has been given to the studies of perturbations of the lower electronic states by the crystalline environment and of the dynamics of relaxation processes in solid matrices.

Photoinduced transformations in molecular complexes is an interesting branch of cryochemistry. The key feature of these investigations is to preliminarily prepare molecular complexes of reactants in the matrix. Further chemical reactions in the complexes are initiated by photo-excitation of one of the reactants. In most cases these studies are limited to identification of reaction products and determination of the relative yields of the principal reaction channels.[55] Description of chemical transformations on the molecular level taking into account the dynamics of molecular rearrangements and the energy relaxation in the lattice is a rather complicated task. Some approaches to the molecular dynamics simulation of these transformations using semiempirical methods of calculations of the PES of corresponding reactions have been reviewed by Raff.[56] If the initial reactants are closed-shell species chemical transformations within the matrix cage will also result in the molecular products. To trap the radical intermediates, the radical fragment of the reacting system should escape the reaction cage and then be trapped outside it. For instance, photodissociation of a complex of a diatomic molecule (AB) with a reactant (M) can yield radical adducts or radical – molecular complexes, if one of the atoms is stabilised outside the reaction cage:

$$[AB\text{---}M] \xrightarrow{h\nu} [A^* + M] + [B^*] \longrightarrow [MA^{\bullet}] + [B_s^{\bullet}], \quad (6a)$$

$$[AB\text{---}RH] \xrightarrow{h\nu} [A^* + RH] + [B^*] \longrightarrow [R^{\bullet}\text{---}AH] + [B_s^{\bullet}]. \quad (6b)$$

However, different research groups (see, *e.g.*, Refs 57–59) reported that photolysis of halogen molecules bound into a complex with the molecules of the other reactant results mainly in the molecular products and that the yield of radical pairs in the reactions (6a) and (6b) is negligible. These results were expected for the complexes containing molecules of heavy halogens (Cl, Br and I). At the same time, the reaction channels (6a) and (6b) can be significant for the complexes with HI (HBr) or F_2 molecules due to weakening of the cage effect for the hydrogen and fluorine atoms compared to the heavy halogen atoms.[60]

Photolysis of isolated molecules in cryogenic matrices is a conventional method of generation of stabilised radicals. Spectro-

scopic data for the radical species thus produced served as the basis for further studies of these objects (see, *e.g.*, Ref. 6). At the same time the cage effect precluding spatial separation of the photodissociation products, the formation of tight radical pairs as well as photolysis of primary products of photodecomposition reduce the efficiency of generation of stabilised radicals and make the interpretation of the spectroscopic and kinetic data more difficult.

Another method for generation of new matrix-isolated particles involves photo-excitation of an isolated particle followed by intramolecular rearrangements. In contrast to the gas phase, photo-excitation to the dissociative absorption band under conditions of the crystalline environment, which impedes spatial separation of the photodissociation fragments, can cause stabilisation of various structural conformers of the same stoichiometry. In most of such studies the molecules were matrix isolated using conventional techniques (see, *e.g.*, Refs 61 and 62). Despite the fact that this procedure for generation of new molecular species has found a rather wide application, there are only a few examples of generation of radical species in this manner. Methodological difficulties in such studies are associated with the necessity of obtaining sufficiently high concentrations of radicals in the absence of other products.

Electronically excited halogen – Rg complexes (Rg is the atom of inert gas) have been traditionally used as a working substance for gas lasers. Basic research into the optical properties of halogen atoms in the solid matrices and crystals of inert gases[63,64] was mainly stimulated by the idea of creation of solid-state excimer lasers. It was found that in most cases the effects of multibody interactions in crystals preclude radiative deactivation of diatomic exciplexes. For instance, the energy of electronic excitation of an ArF complex in solid argon is close to that determined in the gas phase (Fig. 6). However, the excited state undergoes fast relaxation (during $\sim 10^{-13}$ s) into a more stable triatomic exciplex $(Ar_2)^+F^-$ (see Ref. 65). Radiative deactivation of diatomic exciplexes in solid krypton is also preceded by the formation of triatomic excited states, *e.g.*, $(Kr_2)^+F^-$ (see Ref. 66). Since exciplexes are characterised by electron transfer from the halogen atom to the atoms of the inert gas, the equilibrium distances in such structures are much shorter than the van der Waals interatomic distances in the ground electronic state. As a result, radiative deactivation of an electronic excitation causes transformation of a large portion of the exciplex energy (1 to 2 eV) into the kinetic energy of the atoms of the dissociating particle (see Fig. 6). This brings about a unique phenomenon, namely, photoinduced migration of 'hot' fluorine atoms in the crystals of inert gases.[65,66] For instance, experiments on photogeneration of fluorine atoms in argon crystals showed that excitation to the ArF exciplex absorption band with light at $\lambda = 193$ nm upon continuous irradiation of the samples leads to bimolecular recombination of fluorine atoms

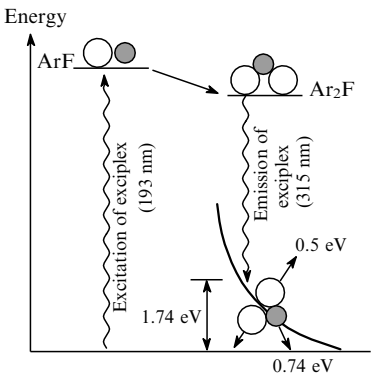


Figure 6. Scheme of excitation and deactivation of ArF exciplex in solid argon.[65]

$$F + F \longrightarrow F_2.$$

The average migration length of a 'hot' F* atom with an initial kinetic energy of ~ 0.7 eV was estimated at ~ 7 nm.[66] An analogous effect of photoinduced migration was also observed for the oxygen atoms isolated in solid krypton or xenon.[67–69] Studies of continuous photolysis of xenon or krypton crystals containing stabilised $O(^3P)$ atoms with light at $\lambda = 248$ nm showed that radiative deactivation of charge-transfer Rg^+O^- exciplexes induces migration of the atomic oxygen in the crystal and, finally, loss of the oxygen atoms by a bimolecular mechanism

$$O + O \longrightarrow O_2$$

Photoinduced migration of reactive atoms in the crystals of inert gases opens up unique prospects for practical implementation of chemical reactions involving these atoms at ultralow temperatures. This is possible if two conditions are met. First, the atom must possess the ability to migrate in the crystal. Second, it must have an excess kinetic energy required to overcome a reaction barrier. Methodologically, there is a feature which complicates a correct interpretation of the results of such experiments. To make atoms mobile, the sample should be irradiated with UV light at a wavelength of about 200 nm. This can cause photoinduced conversions of both the reactant molecules and the primary products of the reactions of the mobile atoms. Nevertheless, this effect can be insignificant since diatomic exciplexes are, as a rule, characterised by extremely large absorption cross sections ($\sim 10^{-16}$–10^{-17} cm^2, see Ref. 66).

III. Translational mobility of hydrogen, fluorine and oxygen atoms in the crystals and solid matrices of inert gases

1. Translationally excited 'hot' atoms produced by photodissociation of isolated molecules

Photodissociation dynamics of small molecules in the crystals of inert gases have been well studied experimentally. Efficient photodecomposition of an isolated precursor can be achieved if the kinetic energy of one reactant (in this case, the atom) is high enough to overcome the lattice barrier which precludes spatial separation of the dissociation products. Possible mechanisms of photodissociation of a number of small molecules, accompanied by generation of H, F and O atoms in the crystals of inert gases, have been considered in detail by Apkaryan and Schwentner.[10] Fundamental difficulties which arise when simulating such processes include the necessity of taking into account the effects of multibody interactions at short distances, which make the pair atom – atom potentials non-additive. Nevertheless, the results of the molecular dynamics simulation are in reasonable agreement with the available experimental data.

The dynamics of 'hot' atoms in the crystal is controlled by the following factors. The $F(^2P)$ and $O(^1D)$ atoms are characterised by relatively short effective interaction ranges in the crystals of inert gases. If such atoms occupy octahedral interstitial sites (O_h) of the f.c.c. crystal lattice, they interact with adjacent lattice atoms (Ar, Kr or Xe) in the attraction region of the pair interaction potentials $U(r)$. At the same time the repulsive part of the interaction potentials at short distances determines the optimum trajectory of the motion of the atom to an adjacent O_h site through the edge of a face of the octahedron.[70,71] Since the masses of the F and O atoms are comparable with those of the atoms of the argon lattice, the energy of a translationally excited 'hot' atom efficiently dissipates by collisions with the lattice atoms. Therefore, efficient escape of the atoms from the cage and spatial separation of the photodissociation products require that the bond cleaved in the photolytic precursor be oriented towards a face of the cell. In this case the atom can migrate in the crystal in a ballistic regime, thus avoiding direct collisions with the lattice atoms.[72]

Quite different are the dynamics of photolytically generated hydrogen atoms. The effective radius of the interaction between the H(^{2}S) atom and Ar, Kr and Xe atoms is comparable with the interatomic distances in the lattice. Therefore, the H(^{2}S) atom interacts with adjacent lattice atoms only in the repulsive region of the pair interaction potentials and the optimum trajectory of the motion of the atom between interstices passes through the centres of the triangular faces of the f.c.c. crystal lattice.[73] It is believed [10] that this predetermines another (compared to the F and O atoms) trajectory of the escape of the 'hot' atom from the reactant cage. In addition, due to the small mass the hydrogen atom loses a small portion of the kinetic energy by collisions with the lattice atoms. Therefore, the requirements on the orientation of the photolytic precursor in the lattice are not so severe as in the case of the F(^{2}P) or O(^{1}D) atoms. In this case the trajectory of motion of the 'hot' hydrogen atom during thermalisation should be close to the diffusion trajectory.

2. Thermally activated diffusion of atoms

Thermally activated mobility of H, O and F atoms in the crystals and matrices of inert gases has been reported by different research groups. The available literature data suggest that fluorine atoms possess extremely high translational mobility in the crystals of argon and krypton. The diffusion coefficients of hydrogen and oxygen atoms have been determined under conditions providing efficient recombination of the atoms, corresponding to typical kinetics of bimolecular reactions. Detailed consideration of these studies is given below.

IV. Chemical reactions involving hydrogen atoms

Hydrogen atoms isolated in cryogenic matrices have been the subject of intensive physicochemical studies using the matrix isolation technique. These investigations were mainly focussed on the problems of creation of high-energy systems, studies of quantum motions of light atoms and on specific features of multibody interactions in the condensed phase. After establishment of the fact that accumulation of high concentrations of stabilised hydrogen atoms in the solid phase is limited due to involvement of these atoms in chemical reactions, the emphasis was placed on the investigation of mechanisms of photoinduced generation of the atoms and subsequent chemical processes with their participation in low-temperature crystals and matrices.

1. Photogeneration of hydrogen atoms

EPR is a very sensitive method for detection of hydrogen atoms in inert matrices. It was found that the lines of the hydrogen doublet in the EPR spectra in solid matrices exhibit a multiplet structure, which is due to the presence of several possible atomic sites in the crystal lattice. Analysis of distortions of the HFC and *g*-factor tensors by the crystal field showed that photogenerated hydrogen atoms are mainly stabilised in the interstitial sites (O_h and T_d) and to a lesser extent in the substitutional sites.[74–78]

The HBr and HI molecules are convenient photolytic precursors for generation of hydrogen atoms in the solid phase. In the early studies (see, *e.g.*, Ref. 6) photolysis of these molecules was used to produce hydrogen atoms that entered into reactions with various reactants. Spectroscopic data for the radical species $HO_2^{\bullet}$, $PHCO^{\bullet}$, $H_2NO^{\bullet}$, *etc.* were first obtained using this experimental technique. It was shown [79] that 'hot' hydrogen atoms produced by photodissociation of HBr in solid xenon are stabilised at rather long distances (up to 10 nm!) from the dissociation site. This conclusion was drawn based on the study of the kinetics of HBr consumption and accumulation of bromine atoms during continuous photolysis of HBr with light at a wavelength of 248 or 193 nm. It was found that the kinetic dependences obey a second-order law due to reactions of the 'hot' atoms (characterised by long migration length) with the distant HBr molecules

$$HBr \xrightarrow{h\nu} Br + H^*, \quad (7)$$

$$H^* + HBr \longrightarrow H_2 + Br. \quad (8)$$

This conclusion was confirmed in a study carried out using the EPR and LIF techniques and molecular dynamics simulation.[78] It was established that only a fraction of photogenerated H atoms is stabilised in the Xe and Kr matrices. Other H atoms either enter into reactions (8) or recombine during thermalisation

$$H + H \longrightarrow H_2.$$

A quite different situation was shown to occur in solid argon where hydrogen atoms are trapped near the dissociation site. Therefore, nearly 100% of the precursor molecules are converted into trapped hydrogen atoms. The molecular dynamics simulation of thermalisation of a 'hot' atom showed that the hydrogen atom with an initial excess energy of 2.5 eV can move from the parent cage over long distances (up to 4 nm in solid krypton). In view of these results, one should expect that reactions of photogenerated 'hot' hydrogen atoms with various molecules should be efficient in solid krypton and xenon.

2. Thermally activated diffusion of hydrogen atoms

Consumption of hydrogen atoms during temperature annealing of solid Rg matrices was reported by different authors.[80–84] It was found that consumption of hydrogen atoms in Kr and Xe matrices at $T > 30$ K obeys a second-order kinetic law, which corresponds to bimolecular recombination. Loss of H atoms in solid argon at temperatures above 12 K was observed. However, analysis of the kinetic dependencies of the loss of H atoms suggested [84] predominance of geminate recombination

$$H + Br \longrightarrow HBr,$$

of the atoms produced during low-temperature photolysis of HBr molecules.

The available literature data allow one to assume that solid matrices of inert gases (Ar, Kr and Xe) can serve as convenient media for studying the interactions of hydrogen atoms with small concentrations of various dopants. Chemical reactions of hydrogen atoms involving cleavage of molecular bonds are, as a rule, characterised by rather high activation barriers ($\geqslant 6-8$ kJ mol^{-1}). At ultralow temperatures, such thermally activated reactions must occur very slowly and therefore the use of photogenerated 'hot' atoms to produce reaction products seems to be more promising than the reactions of diffusing 'cold' atoms. At the same time stabilisation of a long-lived pre-reaction complex H---M formed by collision of the mobile atom with the isolated molecule in the absence of efficient thermal activation of chemical reactions provides the possibility of studying the interactions in the stage where the reactants approach each other.

Studies of tunnelling reactions of hydrogen exchange with hydrogen isotopes in solid hydrogen [85–87] were also carried out in solid argon where the bound state of reactants was first detected by EPR.[88,89] Stable complexes of reactants were formed as a result of diffusion of the H and D atoms at temperatures above 17 K. In particular, the atoms diffusing in solid Ar/HD mixtures form pre-reaction complexes upon collisions with the HD molecules. Among subsequent exchange reactions,

$$D^{\bullet}\text{---}HD \longrightarrow D_2\text{---}H^{\bullet}, \quad (9a)$$

$$H^{\bullet}\text{---}HD \longrightarrow H_2\text{---}D^{\bullet} \quad (9b)$$

a tunnelling transition resulting in complexes of the products is possible only in reaction (9a). This allows one to expect stabilisation of two complexes, $H^{\bullet}\text{---}HD$ and $H^{\bullet}\text{---}D_2$, in this system. Their EPR spectra (Fig. 7) exhibit a resolved HFS on the doublet lines of the H atoms due to the interaction of the unpaired electron of the atom with the magnetic nuclei of the molecules in the complexes $H^{\bullet}\text{---}HD$ and $H^{\bullet}\text{---}o\text{-}D_2$. Besides, the hyperfine splitting on the hydrogen atom in the complex ($a_H = 51.18$ mT) differs from the characteristic a_H values of the atoms trapped in solid

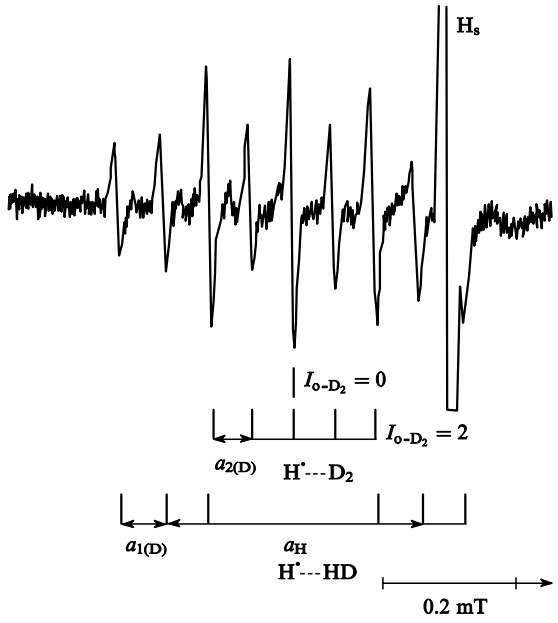


Figure 7. EPR spectra of van der Waals complexes H•---HD and H•---D_2 formed in an argon matrix at 20 K.[89]
The intense line denoted by H_s is due to hydrogen atoms stabilised in the substitutional site O_h. Shown are the characteristic splittings for individual complexes.

argon (a_H = 50.73, 51.42 and 51.54 mT for the substitutional site and the O_h and T_d interstitial sites, respectively).

The spectra of complexes H•---H_2 generated analogously in Ar/H_2 mixtures exhibit no super-HFS since the more stable parahydrogen molecule has a zero nuclear magnetic moment in the ground rotational state. Nevertheless, the formation of this complex was detected by the appearance of the hydrogen doublet with a_H = 51.18 mT. Specific features of the EPR spectra, such as narrow isotropic HFS lines and equal values of the constants of super-HFC with both atoms of the H_2, HD and o-D_2 molecules (with allowance for correction for different gyromagnetic ratios, μ_H/μ_D = 6.5) were attributed to fast internal rotation in the complex. Quantum-chemical QCISD/aug-cc-pvqz calculations of hyperfine interactions in the complex showed that the experimental superhyperfine splitting $a_{H'}$ = 0.386 mT corresponds to a distance of 0.245 nm between the atom and the geometric centre of the molecule.[89] This is much shorter than the value calculated earlier for free van der Waals complex H•---H_2 on the PES of the H_3 system (0.34 nm). These data are in agreement with the results of investigations of tunnelling reactions of H atoms in solid hydrogen (H_2, D_2 and HD), according to which the distances between the reactants in the crystalline environment are shortened.[90]

3. Formation of chemical bonds with atoms of inert gases

A unique feature of heavy atoms of inert gases (xenon and krypton) is their ability to form chemical bonds with other atoms or molecular fragments that are efficient electron acceptors. This is due to a relatively low ionisation energy of the closed-shell atoms. This type of stable compounds can be exemplified by XeF_2 and XeF_4 which were first synthesised more than three decades ago.[91,92] Data on binding xenon atoms into chemical compounds with fluorine and oxygen atoms have been generalised in some reviews (see, *e.g.*, Refs 93–95).

Quantum-chemical calculations predict that the formation of weak chemical bonds with the light atoms of inert gases is possible.[96] Such chemical compounds can be stabilised only at ultralow temperatures. Therefore, the crystals of inert gases, which interact with free atoms under these conditions, are, strictly speaking, not chemically inert. For instance, the $XeCl_2$ and KrF_2 molecules were first synthesised and characterised under matrix isolation conditions.[97–99]

Convincing proofs of the possibility for chemical bonds with the atoms of inert gases were provided by researchers from Finland who detected a number of new chemical compounds, namely, H–Xe–H, H–Xe–Y and H–Kr–Y (Y is the halogen atom or a $CN^•$ or $OH^•$ radical). These compounds are formed in the reactions of diffusing hydrogen atoms in the solid matrices of xenon and krypton.[100–102] Studies of these reactions have been reviewed.[103,104] It is believed that neutral molecules H–Rg–Y are formed as a result of the interaction of two close-lying diabatic PES corresponding to the interaction between neutral and charged fragments (Fig. 8). The low-lying bound state $^1\Sigma^+$ is treated as an ion pair $(HRg)^+Y^-$ in which the covalently bound fragment $(HRg)^+$ is involved in electrostatic interaction with the negatively charged fragment Y^-. Based on this model, a molecular structure with ionic bond, $(HXe)^+Cl^-$, was predicted by semiempirical quantum-chemical calculations even in 1988.[105] The structure H–Xe–H is treated analogously, that is, as a resonance hybrid between $(HXe)^+H^-$ and $H^-(XeH)^+$. Quantum-chemical calculations predict a linear geometry of H–Rg–Y and the molecular energies lying between 38 and 135 kJ mol^{-1} relative to the energy of dissociation into neutral atoms. Global potential minima of such systems correspond to neutral HY molecules and Rg atoms. Because of the ionic type of chemical bonding the molecules H–Rg–Y are characterised by high IR band intensities and by an extremely large dipole moment of the electronic transition $A^1\Sigma \leftarrow X^1\Sigma$ between two close-lying electronic states.[106,107] Therefore, such particles are mostly studied by IR and optical spectroscopy. Table 3 lists the experimental and calculated frequencies of the H–Rg stretching vibrations as well as the calculated bond lengths for a number of compounds.

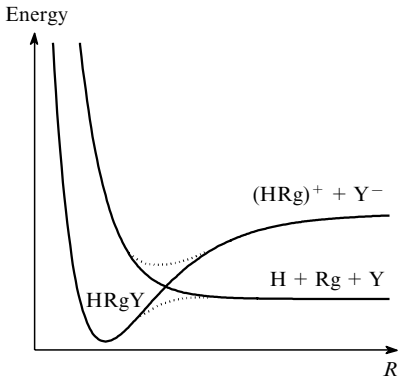


Figure 8. Scheme illustrating the nature of the chemical bond in HRgY molecules. Diabatic PES for the ionic $[(HRg)^+ + Y^-]$ and neutral (H + Rg + Y) states of the system are shown by solid lines.[103]
The abscissa is the sum of the H–Rg and Rg–Y distances in the linear configuration HRgY.

It was also found that HXeOH and HXeH stabilised in solid xenon dissociate over $\sim 10^3$ s at temperatures of 54 and 66 K, respectively.[107] Thermal decomposition was explained by decay of metastable states upon activation of bending vibrations

$$HXeOH \longrightarrow H_2O + Xe \qquad (10)$$

and

$$HXeH \longrightarrow H_2 + Xe.$$

However, no formation of H_2O and H_2 molecules that would provide confirmation of the existence of such a dissociation channel was observed. The energy of IR quantum necessary to decompose a compound by multilevel IR excitation or the long-

Table 3. Experimental and calculated parameters of compounds H – Xe – Y and H – Kr – Y.[103, 104]

Compound	ν_1 /cm^{-1}	ν_2 /cm^{-1}	l_1 /nm	l_2 /nm
H – Xe – Cl	1648	1799	0.1685	0.2663
H – Xe – Br	1504	1730	0.1694	0.2837
H – Xe – I	1193	1560	0.1747	0.3095
H – Xe – CN	1624	1817	0.1707	0.2392
H – Xe – OH	1578	1823	0.1718	0.2208
H – Xe – H	1166/1181 (asym.)	1334 (asym.)	0.1861	–
H – Kr – Cl	1476	1758	0.1435	0.2666
H – Kr – CN	1497	1738	0.1466	0.2349

Notations: ν_1 and ν_2 are the experimental and calculated frequencies of H – Rg vibrations; l_1 and l_2 are the calculated H – Rg and Rg – Y bond lengths, respectively; the bond lengths and vibrational frequencies were calculated at the MP2 level of theory in the harmonic approximation.

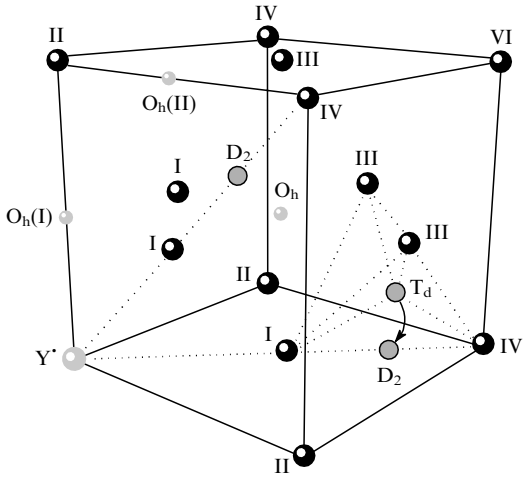


Figure 9. The O_h, T_d and D_2 interstitial sites occupied by hydrogen atom in the f.c.c. crystal lattice of an inert gas.
Impurity particle Y$^\bullet$ occupies the substitutional site. Roman numerals I – IV and VI denote the atoms in the first to fourth and in the sixth coordination spheres of the crystal surrounding the impurity Y$^\bullet$.

wavelength edge in the electronic absorption spectra are used as the upper limit of the binding energies. The H – Rg – Y particles have rather large intrinsic dipole moments; hence, polarisation interactions between them and the surrounding atoms can strongly affect the spectroscopic and energy characteristics of the intermediate. Therefore, the problem of stability of both free and matrix isolated particles is still to be clarified. Currently, the H – Rg – Y particles have been the subject of intensive research [107–109] and one can expect to obtain new data on these interesting objects by the time of publication of this review.

The procedure for generation of the H – Rg – Y particles employed in the above-mentioned studies included (i) preparation of thin films of inert gas, containing a controlled amount of HY molecules (*e.g.*, HI, HCl or HCN), (ii) low-temperature photolysis of the impurity molecules, resulting in the formation of spatially separated radical pairs H$^\bullet \cdots$ Y$^\bullet$ and (iii) annealing of the matrix up to the temperatures at which thermally activated diffusion of hydrogen atoms is possible. The results of a joint study by IR, optical and EPR spectroscopy showed that the kinetics of loss of the hydrogen atoms correlates with the kinetics of formation of the H – Xe – H and H – Xe – Y molecules.[83, 107] In the course of the reactions the loss of the stabilised radicals Y$^\bullet$ amounts to 40%, and virtually no recombination of the molecules of the photolytic precursor HY occurred. With allowance for these facts it was concluded that the three-body interactions H + Rg + H and H + Rg + Y, which are responsible for stabilisation of the xenon- and krypton-containing compounds, are the principal channels of loss of the diffusing atoms. Detailed quantitative balance for the reactions of the diffusing atoms has not been determined as yet; however, the results of kinetic measurements suggest that high-energy processes of direct recombination of the radicals,

$$\begin{aligned} &H^\bullet + H^\bullet \longrightarrow H_2, \\ &H^\bullet + Br^\bullet \longrightarrow HBr, \\ &H^\bullet + Cl^\bullet \longrightarrow HCl, \\ &H^\bullet + CN^\bullet \longrightarrow HCN \end{aligned} \qquad (11)$$

are inefficient under such conditions due to stabilisation of triatomic intermediates H – Rg – Y.

Quantum-chemical calculations of the PES of a free HRgY particle (in the ground electronic state $^1\Sigma^+$) showed that the reaction can follow two routes as the hydrogen atom approaches the RgY fragment. If the angle of attack, H – Rg – Y, is larger than 90° and the H – Rg distance is shorter than 0.4 nm, the system tends to reach an intermediate bound state with a linear configuration H – Rg – Y. In contrast, if the angle of attack is smaller than 90°, the system tends to arrive at a global minimum corresponding to recombination H$^\bullet$ + Y$^\bullet$ (see Refs 103 and 104).

Realisation of a particular reaction channel in the crystal is determined by the trajectory of the motion of the hydrogen atom in the vicinity of the trapped impurity (heavy fragment Y$^\bullet$). Diffusion of hydrogen atoms in the f.c.c. crystal lattice of inert gas has been traditionally treated as random jumps between octahedral interstitial sites O_h, which occur in such a way that in the intermediate states the H atom is located at the tetrahedral site T_d (Fig. 9). If a heavy fragment of primary photodissociation (Y$^\bullet$) occupies a lattice site, recombination H$^\bullet$ + Y$^\bullet$ should occur when the H atom arrives at a tetrahedral T_d (I) or octahedral site O_h(I) adjacent to the fragment Y$^\bullet$. The formation of a bound species H – Rg – Y must occur with participation of an Rg(I) atom (one of the twelve lattice atoms in the first coordination sphere of the Y$^\bullet$ species). Linear structure H – Rg(I) – Y can be formed if the hydrogen atom occupies the interstitial site D_2. There are several T_d and O_h(II) sites outside the first coordination sphere of the Y$^\bullet$ fragment (see Fig. 9). Jumping between them, the hydrogen atom arrives at the attraction region on the PES of the triatomic system H – Rg(I) – Y and becomes bound into the intermediate H – Rg(I) – Y. As a consequence, its recombination with the fragment Y$^\bullet$ is now impossible. If the H atom arrives at other tetrahedral sites T_d surrounding the first coordination sphere of the fragment Y$^\bullet$, the H – Rg$_2$(I) – Y configurations comprised of adjacent atoms are formed.

It is known that cations of the type $(HRg_2)^+$ can be stabilised in low-temperature matrices. Therefore, analogous ionic bonds $(H-Rg_2)^+ - Y^-$ can also be formed in such T_d configurations and these T_d sites can be considered as saddle points for binding the H atom into a more stable linear configuration H – Rg(I) – Y. In this case all trajectories of the H atom, which lead to recombination of fragments, are blocked by the interactions responsible for stabilisation of the intermediate. This treatment demonstrates the necessity of taking into account multibody interactions to gain a deeper insight into the mechanisms of the reactions of diffusing hydrogen atoms with isolated impurity Y$^\bullet$.

The synthesis of a compound called hydrido argon fluoride, H – Ar – F, in solid argon has been reported.[110] Changes in the vibrational frequencies of the stabilised intermediate upon isotope substitutions H → D and ^{40}Ar → ^{36}Ar are thought to be the most important argument in favour of the formation of the H – Ar and F – Ar bonds. According to quantum-chemical calculations carried out at the CCSD(T)/aug-cc-pVQZ level of theory (see Ref. 111), the energy of HArF is 14.7 kJ mol^{-1} relative to the energy of dissociation into neutral atoms while the barrier to

dissociation is 17.2 kJ mol^{-1}. In addition, calculations predicted a high stability of the intermediate towards internal conversion into neutral systems corresponding to the global potential minimum

$$H-Ar-F \longrightarrow HF + Ar.$$

Such a conversion can occur involving the bending vibration. The calculated barrier to reaction along the coordinate of the H – Ar – F bending vibration was ~96.4 kJ mol^{-1}.

Taking into account successful stabilisation of chemical compounds H – Rg – Y (see above), one can suggest that the use of experimental methods employed for the synthesis of such compounds will allow detection of new compounds with the atoms of inert gases including light Rg atoms. Calculations predict that the reaction barriers responsible for the intrinsic stability of such intermediates are at most 10 – 15 kJ mol^{-1}; therefore, stabilisation of these particles requires operation at temperatures below 20 K. Bondybey *et al.*[108] succeeded in using solid neon for stabilisation of intermediate particles (H – Kr – Br) under conditions where thermal diffusion of hydrogen atoms unfreezes at temperatures below 10 K. Low-density solid media (*e.g.*, impurity – helium solid phase, which is stable at temperatures below 10 K) can also be considered as solid matrices suitable for stabilisation of loosely bound compounds of various atoms with the atoms of inert gases.[112, 113] The morphology of such structures is not known with certainty; however, Boltnev *et al.*[114] have demonstrated the possibility of doping solid phases of composition Rg(He)$_n$ (Rg = Ne, Ar, Kr, Xe; $n > 10$) with reactive species.

V. Chemical reactions involving fluorine atoms

Chemical reactions with participation of fluorine atoms have been the subject of intensive basic and applied research.[115, 116] These reactions are characterised by high exothermicity and low energy barriers (usually, the gas-phase barriers are at most 8 kJ mol^{-1}), which predetermines high reaction rates and the formation of excited products. The matrix isolation technique has been traditionally used for detection and studies of the products of such reactions. Comprehensive reviews of investigations in this field carried out to the late 1980s have been reported by Jacox.[6, 117] Because of this we will concern ourselves with more recent studies.

1. Translational mobility of fluorine atoms

The unique properties of fluorine atoms produced by photodissociation of F_2 molecules isolated in solid argon or krypton matrices have been reported in the early 1990s. Experiments[66] showed that the quantum yield of photodissociation of F_2 is close to unity, if the excess energy per atom,

$$\Delta E = \frac{h\nu - D_e(F_2)}{2},$$

where D_e is the dissociation energy of the F_2 molecule, exceeds 1 eV. As can be seen from Fig. 10, at $\Delta E > 1$ eV the cage effect is insignificant and the efficiency of photodissociation of F_2 in solid argon is close to the efficiency of the corresponding gas-phase process. Photodissociation of F_2 in solid matrices is basically different from the photodissociation of the molecules containing heavy halogens (Cl_2, ICl, Br_2), since in the latter case the quantum yield is at most 10^{-5} at moderate excess energies (< 3 eV).[118–120] The thermalisation length of a 'hot' atom F was estimated at 3 – 8 nm.[66]

The possibility for a long-range migration of 'hot' fluorine atoms to occur was also confirmed by other researchers,[121] though estimates of the thermalisation length were smaller. Using the molecular dynamics simulation, it was shown [72] that migration of a 'hot' atom in the crystal occurs as ballistic motion (*i.e.*, the trajectory of the fluorine atom passes through the lattice interstices) until the first strong collision with the lattice atom. This is due to efficient dissipation of the energy of the 'hot' fluorine atom in the interaction with the argon atoms. Yet another feature of the fluorine atoms is that their diffusion mobility unfreezes at temperatures much below the melting (sublimation) temperature of the crystal. Consumption of the fluorine atoms produced by photolysis of F_2 in the crystals of argon and krypton is illustrated in Fig. 11. At concentrations of the order of 10^{17} cm^{-3}, the lifetime of the F atoms stabilised in argon is nearly 10^3 s at 20 K. Kinetic measurements revealed the absence of geminate recombination of the atoms produced by photodissociation of one F_2 molecule.[66] In the course of diffusion the atoms migrate in the crystal over long distances and the kinetics of loss of the atoms corresponds to bulk recombination

$$\frac{d[F]}{dt} = -k_d[F]^2, \qquad (12)$$

where [F] is the volume average of the concentration of the atoms.

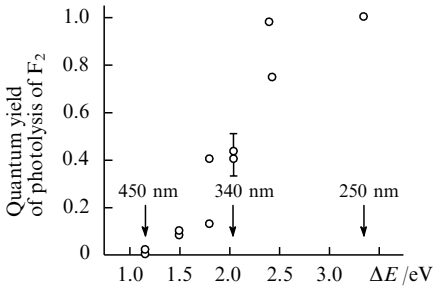


Figure 10. Quantum yield of photodissociation of F_2 molecules isolated in solid argon as a function of excess photon energy.[66]
The arrows denote the characteristic wavelengths of photolysing radiation.

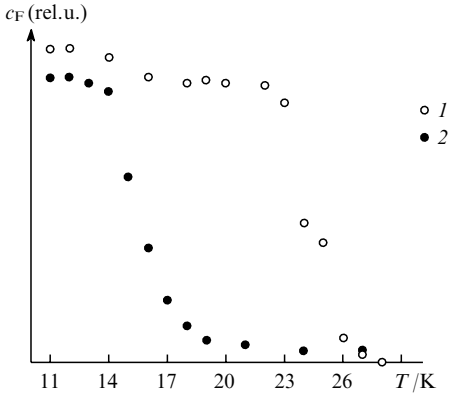


Figure 11. Temperature dependence of the concentration of fluorine atoms (c_F) in argon (*1*) and krypton (*2*) crystals.[66]
Heating of samples from 10 K at a rate of ~0.5 K min^{-1}.

2. Reactions of photogenerated 'hot' fluorine atoms

As photogenerated 'hot' atoms escape the parent cage, they can react with distant molecules of the other reactant. The formation of stabilised radicals generated by low-temperature photolysis of solid Rg/F_2/M mixtures was established in the early studies (see, *e.g.*, Refs 33, 35, 122, 123). However, no reaction channels responsible for the formation of such products were found. The point is that the radical species can be produced both in the interaction of the migrating atom with the isolated impurity molecule, F + M, and by photolysis of F_2 contained in heterodimers [F_2 --- M], if the photogenerated atom escapes the cage [see reactions (6a) and (6b)]. However, in a series of studies [58, 124, 125] it

was shown that photolysis of heterodimers [F_2---M] results in predominant formation of molecular (closed-shell) products. Therefore, the emphasis was placed on studies of hydrogen-bonded molecular complexes generated in photoinduced reactions

$$[F_2\text{---}H_2] \xrightarrow{h\nu} [HF\text{---}HF], \quad (13a)$$

$$[F_2\text{---}CH_4] \xrightarrow{h\nu} [CH_3F\text{---}HF], \quad (13b)$$

$$[F_2\text{---}NH_3] \xrightarrow{h\nu} [NH_2F\text{---}HF]. \quad (13c)$$

In our joint investigations carried out in collaboration with Prof. C Wight (University of Utah, USA) we succeeded in distinguishing between the reaction channels associated with the formation of molecular and radical products in such systems.[20, 21] Figure 12 presents the kinetic curves of consumption of the reactants and of accumulation of the products during photolysis of Ar/F_2/CO mixtures prepared using a conventional matrix isolation technique. Exponential fit of the kinetic curves of consumption of the CO molecules and binary complexes [F_2---CO] in the course of continuous photolysis shows a nearly twofold difference in the rates of the processes. The rate of accumulation of the F_2CO molecules equals the rate of consumption of the [F_2---CO] complexes, whereas an increase in the concentration of the FCO$^{\bullet}$ radicals correlates with consumption of isolated CO molecules. Spectral and kinetic studies of the reactants and reaction products revealed two principal reaction channels with participation of photogenerated fluorine atoms:
(1) reaction in the complex of reactants

$$[F_2\text{---}CO] \xrightarrow{h\nu} F_2CO; \quad (14)$$

(2) reaction of a 'hot' F* atom with an isolated CO molecule

$$[F_2] \xrightarrow{h\nu} F^* + F^*, \quad (15)$$

$$F^* + CO \longrightarrow FCO^{\bullet}. \quad (16)$$

Analysis of changes in the band intensities in the IR spectra of the reactants and reaction products showed that the mass balance for consumption of complexes [F_2---CO] and accumulation of F_2CO is kept constant within the limits of experimental error (±10%). This means that photolysis of complexes of the reactants causes no exit of the fluorine atoms from the reaction cage; rather, they react with the neighbouring CO molecule. Only ~3% of the CO molecules in the samples of composition Ar : F_2 : CO = 1000 : 1 : 1 undergo conversion into the FCO$^{\bullet}$ radicals following reaction (16). The proportion of binary complexes [F_2---CO], which produce the F_2CO molecules in reaction (14), is ~7% – 10% of the total amount of CO molecules. Thus, the amount of molecular products of the cage reaction exceeds the amount of radicals generated in the reactions of the migrating 'hot' fluorine atoms by a factor of 2 to 3. This product ratio remains unchanged for the samples of various compositions (at x_{F_2} and $x_{CO} < 10^{-3}$), since the amounts of the radical products and [F_2---CO] complexes vary in proportion to the concentrations of F_2 and CO in the sample. Analogous measurements were also carried out in argon crystals doped with F_2 and CO molecules.[21] The principal channels of the reactions of photogenerated atoms in the crystal and in the argon matrix were found to be similar. However, a basic difference between them is that the yield of radicals in reaction (16) in the crystal was 10 to 15 times higher than in the matrix at equal initial concentrations of the reactants in the samples.

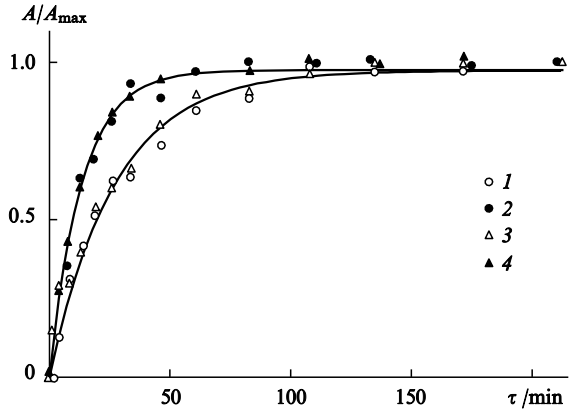


Figure 12. Kinetic curves of consumption of CO molecules (*1*) and [F_2---CO] binary complexes (*2*) and those of accumulation of reaction products for FCO$^{\bullet}$ radicals (*3*) and F_2CO molecules (*4*) during continuous photolysis of a ternary sample (Ar : F_2 : CO = 2000 : 1 : 1) with light (λ = 355 nm) at 16 K.[20]
The experimental band intensities were normalised to their values after 215 min of photolysis. The curves denote exponential fits to the experimental data.

The ratio of the amount of radicals produced to the initial amount of F_2 molecules in the sample was used [20, 21] as a measure of the efficiency of reaction (16) between the migrating F* atoms and the isolated molecules. If the relative concentration of the molecules of the second reactant, x_m, is less than 10^{-2}, this ratio increases in proportion to x_m for all the systems studied

$$\frac{[R]}{[F_2]_0} = Kx_m, \quad (17)$$

where K is the coefficient characterising the yield of stabilised radicals in the reactions of photogenerated fluorine atoms with impurity molecules in the solid argon matrix.

The coefficient K determined from the concentration dependencies for reactions of F* atoms with CO molecules in an argon matrix was found to be 27 ± 8. Analogous measurements in argon crystals gave a much larger value, 340 ± 120. Even with allowance for the error of measurements the efficiency of the reaction of 'hot' fluorine atoms in argon crystal is more than an order of magnitude higher than in the matrix.

The coefficient K characterises the number of lattice atoms which are 'surveyed' by two migrating, photogenerated fluorine atoms (in order to react with impurity molecule). This value must depend on both the mean thermalisation length, $\langle l \rangle$, and the reaction cross-section, σ_m. The reaction of the thermalised atom with the nearest environment should also be taken into account. If migration occurs in the ballistic regime up to the first strong collision followed by thermalisation [72] (provided a uniform distribution of reactants over the sample), the yield of radicals can be evaluated from the simple expression

$$\frac{[R]}{[F_2]_0} = (2\sigma_m \langle l \rangle N_0 + 2Z)x_m, \quad (18)$$

where N_0 is the density of atoms in the argon crystal and $Z = 6$ is the coordination number for the O_h interstitial site in the crystal.

According to Eqn (18), the maximum value, K(matrix) ≃ 50, corresponds to a mean thermalisation length of the atom of $\langle l \rangle \simeq 1.5$ nm, or nearly three lattice constants of the argon crystal. A higher yield of radicals in the crystal can be due to a much larger $\langle l \rangle$ value compared to the matrix. The mean thermalisation length in the crystal estimated from the experimental K(crystal) value is as long as 17 nm. Expression (18), as applied to the atomic dynamics in the solid phase, is not rigorous since the atom moves in the crystal field and continuously loses its energy. Therefore, these $\langle l \rangle$ values should be treated as estimates. Nevertheless, they are in agreement with the results of earlier studies in which different scales for migration of 'hot' atoms in argon crystals and in solid matrices were obtained.[66, 121] The relatively low reactivity of such atoms in the matrix can be rationalised by shortening of the thermalisation length due to the small size of crystallites and to high concentration of defects. Taking into

account the mass ratio of the F and Ar atoms, one can suggest that the fluorine atom with an initial energy of ~ 1 eV must undergo thermalisation after 1–3 successive collisions with the lattice atoms. Without considerable loss of energy the 'hot' atom can migrate in the crystal only by moving along specific trajectories passing through the interstices of the crystal lattice, thus avoiding strong collisions with the lattice atoms. Only in this case can the migration length of a 'hot' atom be as long as ~ 10 nm,[72] the lattice defects being a 'heat sink' for the excess energy of the atom, thus accelerating its thermalisation in the matrix.

Table 4 lists the K values measured in an argon matrix for the reactions of 'hot' fluorine atoms with various molecules. The most efficient is the interaction of such atoms with small diatomic molecules; the interaction with large molecules (*e.g.*, C_2H_2 or C_2H_4) is 2 to 3 times less efficient. Hydrogen abstraction reactions are characterised by the smallest K values. In contrast to nearly barrierless reactions of addition to diatomic molecules O_2, CO, NO (energy barriers to these reactions in the gas phase are at most 2 kJ mol^{-1}), the barriers to hydrogen abstraction from NH_3, CH_3 and H_2 molecules in the gas phase vary from 4 to 7.5 kJ mol^{-1}. An important factor, which also reduces the probability for the 'hot' atom to react, is high stereospecificity of the hydrogen abstraction reactions in which the atom must attack the molecule along the C–H bond (collinear collision).

Table 4. Values of K coefficient in formula (17).

Reaction	Products	K	Measuring technique
$F + O_2$	$FO_2^{\bullet}$	45 ± 13	IR spectroscopy
		29 ± 8	EPR
$F + CO$	$FCO^{\bullet}$	27 ± 8	IR spectroscopy
		19 ± 5	EPR
$F + NO$	FNO	24 ± 7	IR spectroscopy
$F + O_3$	$FO_3^{\bullet}$	22 ± 7	"
$F + C_2H_2$	$2\text{-}C_2H_2F^{\bullet}$	15 ± 4	"
$F + C_2H_4$	$2\text{-}C_2H_4F^{\bullet}$	11 ± 3	EPR
$F + NH_3$	$H_2N^{\bullet}\cdots HF$	3.8 ± 1.0	IR spectroscopy
$F + CH_4$	$H_3C^{\bullet}\cdots HF$	1.8 ± 0.5	EPR
$F + H_2$	$H^{\bullet}\cdots HF$	0.9 ± 0.3	"

3. Reactions of diffusing fluorine atoms

Thermally activated chemical reactions in thin argon films doped with fluorine atoms and molecules of the second reactant have long been observed (see Refs 6 and 117). Transformations observed were explained by unfreezing of the local mobility of the atoms at high temperatures. More recent studies revealed a key feature of the diffusing atoms, namely, the absence of geminate recombination of photogenerated atoms and the ability of such atoms to diffuse over long distances in crystals and argon matrices.[65,66] In this case chemical reactions of mobile atoms are limited to their bulk recombination [see Eqn (2a)]. Assuming a uniform distribution of molecules throughout the sample, the kinetics of processes can be described using the volume averaged concentrations of reactants and the rate constants for bimolecular reactions (2a) and (2b). In the framework of this approach the efficiency of reactions of diffusing atoms can be characterised by the ratio of the concentration of radicals produced to the initial concentration of atoms [126]

$$\frac{[R]_{max}}{[F]_0} \cong \frac{k_r}{k_d}\frac{[x_m]_0}{[F]_0}\ln\left(1+\frac{k_d}{k_r}\frac{[F]_0}{[x_m]_0}\right), \qquad (19)$$

which is in turn determined by the ratio of the initial concentrations of the reactants, $[F]_0/[x_m]_0$, and by the ratio of the rate constant for reaction (2b) to the rate constant for recombination of atoms (2a), k_r/k_d. The k_r/k_d ratios for various reactions are listed in Table 5. As can be seen, the values of this parameter vary by three orders of magnitude. The O_2 and CO molecules are the most efficient scavengers of diffusing atoms. The rate constants for the reactions with these molecules are close to the rate constant for recombination of the atoms. The smallest k_r/k_d values were obtained for the reactions of hydrogen abstraction from the CH_4 and H_2 molecules.

Table 5. The k_r/k_d ratios for reactions of thermal fluorine atoms in an argon matrix at 26 K. (The recombination constant of F atoms is $\sim 2 \times 10^{-21}$ cm^3 s^{-1} at 26 K.)

Reaction	k_r/k_d	Measuring technique
$F + CO$	0.4–0.6	IR spectroscopy
	0.35–0.45	EPR
	0.45–0.6	IR spectroscopy in crystal
$F + O_2$	0.6–0.8	IR spectroscopy
	0.5–0.65	EPR
$F + C_2H_4$	0.2–0.3	IR spectroscopy
	0.15–0.25	EPR
$F + NH_3$	0.02–0.03	"
$F + CH_4$	0.001–0.002	"
$F + H_2$	0.0003–0.001	"

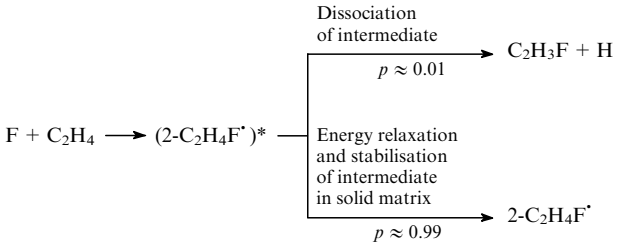
An example illustrating the efficiency of stabilisation of the reactive intermediate in the matrix is provided by the interaction $F + C_2H_4$, resulting in addition of fluorine at the double bond of ethylene and the formation of a vibrationally excited radical

$$F + C_2H_4 \longrightarrow (2\text{-}C_2H_4F^{\bullet})^* + 210 \text{ kJ mol}^{-1}. \qquad (20)$$

In the gas phase the radical dissociates in $\sim 10^{-9}$ s (see Ref. 127)

$$(2\text{-}C_2H_4F^{\bullet})^* \longrightarrow C_2H_3F + H - 150 \text{ kJ mol}^{-1}. \qquad (21)$$

Stabilisation of $2\text{-}C_2H_4F^{\bullet}$ in the matrix requires transfer of an energy of ~ 60 kJ mol^{-1} into the matrix, the transfer time being shorter than the dissociation time. In contrast to the gas-phase reaction, the reaction of diffusing fluorine atoms in solid argon results in stabilised intermediate as the major product.[39,128,129]



p is the reaction channel probability.

High resolution of the HFS in the EPR spectra of isolated radicals $2\text{-}C_2H_4F^{\bullet}$ allowed detailed analysis of the spectra and determination of the character of internal motions in the stabilised radical. Eight vibrational frequencies of this radical were first determined by IR spectroscopy.[129]

New reactive intermediates generated in solid-phase reactions of mobile fluorine atoms are considered below.

4. Radical–molecular complexes $R^{\bullet}\cdots HF$

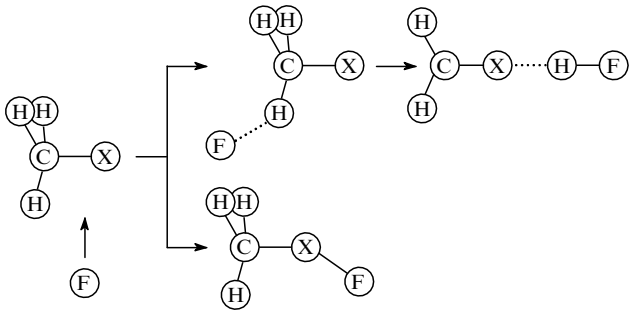
According to published data obtained from studies in the gas phase and from quantum-chemical calculations, most hydrogen abstraction reactions

$$F + RH \longrightarrow R^{\bullet} + HF \qquad (22)$$

occur in a collinear complex where the fluorine atom attacks the reactant molecule along the R–H bond.[130,131] No bound intermediate states of such reactions were observed earlier, though the possibility for them to exist in the vicinity of the transition state both in the product and the reactant valleys was discussed in the literature. Different ways of trapping the products of chemical

reactions (22) in low-temperature matrices have been considered.[117] It was pointed out that stabilisation of the bound state of products, R•---HF, can be achieved only if the solid-phase reaction is carried out. Information on such complexes provided by IR spectroscopy is insufficient. High-frequency vibrations of radicals change only slightly upon binding into complexes, while the frequencies of characteristic intermolecular vibrations in the complexes appear in the region below 300 cm^{-1} and are unavailable for conventional measuring techniques. The frequency shift of the HF stretching vibration (difference between the frequency in complex and the vibrational frequency of isolated HF molecule) can be indicative of binding the molecule into complex. However, it provides only qualitative information on the binding energy of the complex.

The possibility of stabilisation of pre-reaction complexes F---RH was shown taking low-temperature co-condensation of fluorine atoms and CH_3X (X = Cl, Br, I) molecules in excess of argon as an example. The processes with participation of these reactants, occurring in the solid matrix, can be schematically depicted as follows:[132]



Complexes H_3CX---F are the major products. Weak additional satellite IR bands characterised by small frequency shifts relative to the intense bands of isolated CH_3X molecules were assigned to the pre-reaction complexes F---HCH_2X. No reactions with participation of CH_3X in the ground electronic state were observed; however, photolysis of the samples by visible light ($\lambda > 420$ nm) led to disappearance of complexes F---HCH_2X and production of complexes $H_2XC^{\bullet}$---HF. The experimental HF vibrational frequencies in a number of related radical–molecular complexes isolated in a solid argon matrix are listed in Table 6. This seems to be the only spectroscopic characteristic of intermediates obtained under such experimental conditions by IR spectroscopy.

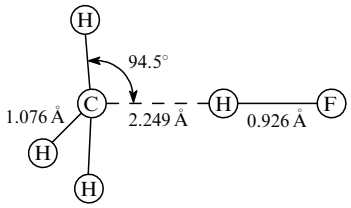
Table 6. HF stretching vibration frequencies (cm^{-1}) of complexes R•---HF and M---HF trapped in a solid argon matrix. (The stretching vibration frequency of HF molecule trapped in a solid argon matrix is 3916 cm^{-1}).

Complexes	Frequency	Ref.
NC•---HF	3753	133
$HC_2^{\bullet}$---HF	3756	133
$H_2FC^{\bullet}$---HF	3854	134
$H_3C^{\bullet}$---HF	3764	24, 135
$H_2N^{\bullet}$---HF	3267	47
HF---HF	3825	136
HCN---HF	3626	137
H_3N---HF	3041	138

A radical–molecular complex $H_3C^{\bullet}$---HF was stabilised in solid argon and identified by IR spectroscopy as an intermediate of the reaction F + CH_4.[135] Experiments with isotope substitution of the reactants ($CH_4 \rightarrow CD_4$) permitted the determination of the HF vibrational frequency (3764 cm^{-1}) and the frequency of the CH_3 out-of-plane vibration (664 cm^{-1}) in the complex. Both vibrations in the complex are characterised by rather large frequency shifts relative to the frequencies of the corresponding vibrations of isolated HF molecule and $CH_3^{\bullet}$ radical (3916 and 619 cm^{-1}, respectively).

The assignment of these frequencies to complexes $H_3C^{\bullet}$---HF generated in the reactions of diffusing fluorine atoms with CH_4 molecules in solid argon was confirmed in more recent IR and EPR studies.[24, 126]

Using the EPR technique it was found that reactions of 'hot' fluorine atoms with isolated CH_4 molecules result in isolated radicals $CH_3^{\bullet}$ as the major product (quartet of HFS lines with the splitting a_H = 2.3 mT). The reactions of diffusing fluorine atoms give a product characterised by a sixteen-component EPR spectrum. Each component of the HFS of radical $CH_3^{\bullet}$ is additionally split into four components due to interaction between the unpaired electron and the magnetic nuclei of the HF molecule (a_F = 1.6 mT, $a_{H'} \leqslant 0.2$ mT). The structure of free complex $H_3C^{\bullet}$---HF corresponding to the bound state on the PES in the product valley has been calculated.[25]



a (calculated) /mT	−2.8	0.3	1.6
a (experimental) /mT	| 2.3 |	⩽ | 0.2 |	| 1.6 |

According to calculations, the complex has a collinear configuration of C_{3v} symmetry and a binding energy of ~8.4 kJ mol^{-1}. The frequency of intermolecular vibration in the complex is 125 cm^{-1} while the frequency of the H–F vibration in the complex is ~130 cm^{-1} lower than in the free molecule. The calculated IHFC constants of the complex are in good agreement with the experimental values. The IHFC constants of the F and H atoms dramatically decrease upon small variations of orientation of the HF molecule relative to the equilibrium configuration. Therefore, it was concluded that most of the reaction products are stabilised in the form of collinear complex $H_3C^{\bullet}$---HF. This lattice-stabilised complex of reaction products retains the symmetry of the transition state of the reaction.

Gas-phase chemical reaction

$$F + H_2 \longrightarrow FH + H, \quad \Delta H_0^{\circ} \approx -134.5 \text{ kJ mol}^{-1} \qquad (23)$$

has been the subject of numerous studies aimed at investigating the reaction dynamics in elementary chemical processes (see, *e.g.*, Refs 139–141). Quantum-chemical calculations[142] predicted a collinear configuration of complex H•---HF in the output channel of the reaction. The authors[142] pointed out that the presence of such a bound state in the product valley affects the angular and energy distribution of the end reaction products. Complex H_2F produced in the reactions of diffusing fluorine atoms with H_2 molecules was first studied experimentally in solid argon by EPR spectroscopy.[143] Two bound configurations of the complex were shown to exist. Their relative concentrations vary in the temperature range from 10 to 30 K due to hindered internal rotation of the HF molecule. Temperature dependence of the shape of the EPR spectra was described using a model with allowance for exchange between the energetically inequivalent configurations of the complexes A → B and B → A. The IHFC on ^{19}F and ^{1}H nuclei of the HF molecule were found to be a_F = 3.2 and $a_H < 0.1$ mT for complex A and a_F = 0.5 and $a_H \simeq 0.4$ mT for complex B. Complex B appears to be more stable, since its contribution to the EPR spectrum increases as the temperature decreases.

Figure 13 presents the isolines of the constants of IHFC with the nuclei of fluorine atoms of the HF molecule calculated for different configurations of the complex. The experimental IHFC a_F and a_H of complex B are consistent with collinear configura-

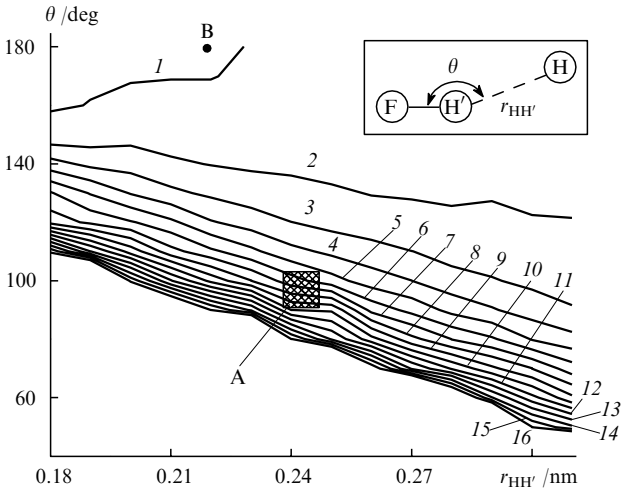


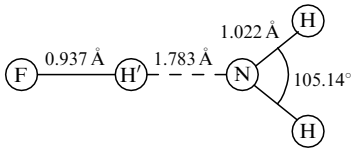
Figure 13. Isolines of IHFC constants on the ^{19}F nucleus in radical–molecular complex H•---HF obtained from B3LYP/aug-cc-pVTZ calculations.
The regions corresponding to the measured IHFC constants are labelled A and B; −0.46 (*1*), −0.05 (*2*), 0.27 (*3*), 0.75 (*4*), 1.82 (*5*), 2.33 (*6*), 2.70 (*7*), 2.83 (*8*), 2.92 (*9*), 3.16 (*10*), *3.44* (*11*), 4.07 (*12*), 4.39 (*13*), 4.49 (*14*), 4.70 (*15*) and 4.71 (*16*).

tion H•---HF with a $r_{HH'}$ distance of 0.22 nm, which corresponds to a local minimum in the product valley on the PES of the reaction.[142] The nature of the second configuration of the complex (A) is still unknown. The experimental IHFC constants of this complex are in agreement with the calculated IHFC constants for a bent configuration H•---H−F characterised by the angle $\theta \simeq 100^\circ$ and the distance $r_{HH'} = 0.24$ nm. We were unable to find in the literature reliable computational data that would help to decide between the presence or absence of the bound state on the PES in this region of geometric parameters of the system.

Interest in gas-phase reaction

$$F + NH_3 \longrightarrow HF + {}^{\bullet}NH_2, \quad \Delta H_0^\circ \approx -130 \text{ kJ mol}^{-1} \qquad (24)$$

was due to attempts at implementing the process in gas lasers to create an inverse population of rovibrational states of HF molecules. However, no inverse population could be created despite the high exothermicity of the reaction.[144, 145] The existence of a strongly bound complex in the output channel of the reaction was predicted theoretically and discussed in the literature based on indirect gas-phase kinetic data.[146] Complex $H_2N^{\bullet}$---HF was first stabilised in solid argon as a product of reactions of mobile fluorine atoms with NH_3 molecules.[46, 47, 147] Table 7 lists the spectroscopic characteristics of the complex, obtained by EPR and IR spectroscopy as well as the results of quantum-chemical calculations, which predict that the free complex has a planar structure of C_{2v} symmetry



The N---H′ binding energy in the complex is 51.5 kJ mol^{-1}. Comparison of the experimental and calculated vibrational frequencies and IHFC constants reveals good agreement between them. The calculated binding energy of the complex is comparable with those of strongly bound hydrogen-bonded molecular complexes (*e.g.*, H_3N---HF). This conclusion is confirmed by the IR spectrum of the complex: a large shift of the HF vibrational frequency and intense librations with frequencies lying between ~800 and 900 cm^{-1} (see Table 7) are characteristic of the

Table 7. Calculated and experimental vibrational frequencies and IHFC constants of radical–molecular complex $H_2N^{\bullet}$---HF.[47]

Parameter (vibration)	Calculated [a]	Experimental
Vibrational frequency /cm^{-1}		
$1a_1$ (HF stretching)	3486	3267
$2a_1$ (NH_2 stretching symmetrical)	3401	–
$3a_1$ (NH_2 scissoring)	1527	1512
$4a_1$ (NH′ intermolecular)	257	–
$1b_2$ (NH_2 stretching asymmetrical)	3497	3211
$2b_2$ (HF in-plane libration)	860	797
$3b_2$	221	–
$1b_1$ (HF out-of-plane libration)	817	791
$2b_1$	280	–
IHFC constant /mT		
a_N	1.15	|1.20|
a_F	−0.70	|0.70|
a_H	−2.30	|2.40|
$a_{H'}$	0.02	< |0.05|

[a] Obtained from B3LYP/EPR-III calculations in the harmonic approximation.

complexes with the binding energies of ~50–70 kJ mol^{-1}. According to quantum-chemical calculations, even small distortions of the geometry of the complex must cause significant changes in the IHFC constants. Taking into account the results of geometry optimisation and the arrangement of the complex at the substitutional site of the argon lattice, it was concluded that the geometry of the complex stabilised in solid argon is similar to that calculated for free complex (Fig. 14).

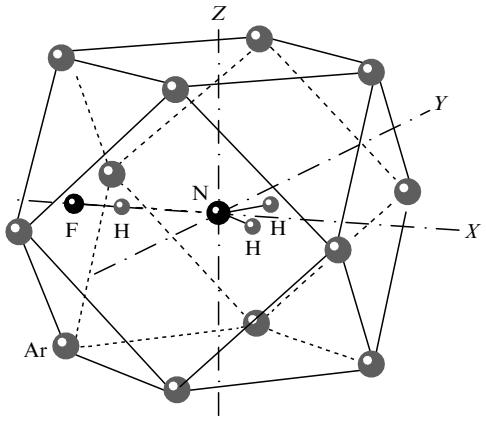


Figure 14. Arrangement and equilibrium geometry of radical–molecular complex $H_2N^{\bullet}$---HF in the argon crystal lattice.[47]
Shown are twelve nearest Ar atoms.

5. Radical $F_2NO^{\bullet}$

Fox *et al.*[148, 149] postulated the formation of a radical species $F_2NO^{\bullet}$ in the synthesis of F_3NO molecules

$$F + NO \longrightarrow FNO, \qquad (25)$$

$$FNO + F \longrightarrow F_2NO^{\bullet}, \qquad (26)$$

$$F_2NO^{\bullet} + F \longrightarrow F_3NO. \qquad (27)$$

Vibrationally excited radical $F_2NO^{\bullet}$ was considered [150] as an intermediate species in other chemical reactions, *e.g.*,

$$O + NF_2 \longrightarrow (ONF_2)^* \longrightarrow FNO + F, \qquad (28)$$

$\Delta H_0^\circ \approx -277$ kJ mol^{-1}.

Attempts at detecting this species experimentally in the elementary reactions (25) – (27) failed. The EPR spectra of radical $F_2NO^\bullet$ were obtained in the experiments on radiolysis of solid F_3NO.[151] This species was stabilised in solid argon (radical was generated in successive reactions of diffusing fluorine atoms with isolated NO molecule).[152,153] IR and EPR spectroscopic studies revealed that in the temperature range 17 – 35 K the radical $F_2NO^\bullet$ exists in dynamic equilibrium with the pre-reaction complex F---FNO

$$F\text{---}FNO \underset{k_-}{\overset{k_+}{\rightleftharpoons}} F_2NO^\bullet. \qquad (29)$$

At high temperatures, the equilibrium is shifted to the right, while at low temperatures it is shifted to the left. The enthalpy and entropy of direct reaction (28) determined using a linear approximation of the temperature dependence of the experimental equilibrium constant are respectively

$$\Delta H = 1240 \pm 180 \text{ J mol}^{-1}, \qquad (30)$$
$$\Delta S = 62 \pm 10 \text{ J mol}^{-1} \text{ K}^{-1}$$

per mole of reactants isolated in solid argon. This indicates that the formation of the second N – F bond in radical $F_2NO^\bullet$ in the solid-phase reaction is an endothermic process. At the same time the formation of this radical is accompanied by a substantial increase in entropy. It is the large positive entropy of reaction (29) that plays a key role in stabilisation of a high equilibrium concentration of radicals upon warm-up of the system when $T\Delta S > \Delta H$. Radicals $F_2NO^\bullet$ can also be detected at $T < 20$ K, since the characteristic time of their dissociaition at these temperatures exceeds 10 h.

A feature of the electronic structure of radical $F_2NO^\bullet$ is that it is characterised by low energy of the N – F bond and a rather high N – F stretching vibration frequency (> 700 cm^{-1}). Because of this, reasonable agreement between the calculated and experimental vibrational frequencies can be obtained only using computational methods with correct inclusion of configuration interactions [QCISD(T)].[153] According to calculations, the N – F bond dissociation energy is merely ~ 10 kJ mol^{-1}. However, the formation of $F_2NO^\bullet$ in solid-phase reaction (29) is endothermic (by 1.2 kJ mol^{-1}). Direct comparison of these two values is impossible, since the initial reactant in the solid-phase reaction was the bound complex F---FNO, whereas the bond dissociation energy was calculated relative to the noninteracting reactants F and FNO. In addition, one should take into account the interaction of the reactants with the atoms of the argon lattice, which must be different for complex F---FNO and radical $F_2NO^\bullet$.

6. Complex FO---O_2

Asymmetric chlorine trioxide $ClO_3^\bullet$ was postulated[154,155] as a reactive intermediate and unstable product of photodecomposition of ozone by chlorine. However, it is impossible to draw unambiguous conclusions about the stability of such intermediates based on the results of quantum-chemical calculations.[156] The assumption of the existence of a bound particle FO_3 was never made in the experimental and theoretical studies of fluorine oxides $FO^\bullet$, $FOO^\bullet$, FOF, OFO and FOOF. It was found that a product of the reaction F + O_3 in photolysed solid $Ar/F_2/O_3$ mixtures is characterised by two intense IR bands at 968 and 1522 cm^{-1} in the region of the vibrational frequencies of FO and O_2, respectively.[157] In the experiments with ^{18}O-enriched ozone these bands were assigned to the F – O and O – O vibrations of reactive intermediate F – O---O – O. Based on the results of kinetic measurements and spectroscopic data, it was concluded that reactions of translationally excited and diffusing fluorine atoms with O_3 molecules result in a highly reactive complex FO---O_2. However, at present the results of quantum-chemical calculations prevent us from drawing unambiguous conclusions about the nature of chemical bonding and the geometry of the complex.

7. Structural isomers of [HFCN]$^\bullet$

The possibility of the existence of two structural isomers in radical systems containing the CN group (*e.g.*, $H_2C=N^\bullet$ and $HC^\bullet=NH$, $F_2C=N^\bullet$ and $FC^\bullet=NF$, $HFC=N^\bullet$ and $FC^\bullet=NH$) was predicted by numerous quantum-chemical calculations.[158–160] However, detailed experimental studies were carried out only for π-radicals $H_2C=N^\bullet$ and $F_2C=N^\bullet$ (see, *e.g.*, Refs 161 – 165). Therefore, quantum-chemical calculations of the structure and properties of such types of radicals are well substantiated experimentally. Until recently, almost no data on free σ-radicals $HC^\bullet=NH$, $FC^\bullet=NF$, $FC^\bullet=NH$ were available. It was assumed[162,163,166] that radicals $HC^\bullet=NH$ and $FC^\bullet=NF$ can be the secondary products of photolysis of solid mixtures Ar/HI/HCN and Ar/*trans*-N_2F_2/FCN. The band at 886 cm^{-1} in the IR spectrum was assigned to radical $HC^\bullet=NH$ while the band at 1053 cm^{-1} was assigned to radical $FC^\bullet=NF$. This assignment is tentative, since it is to a great extent based on the experience and professional intuition of researchers.

Recent EPR and IR spectroscopic studies[167,168] allowed the conditions for stabilisation of radical conformers $HFC=N^\bullet$ and $FC^\bullet=NH$ in solid argon to be determined for the first time. It was shown that a π-radical is generated in the reaction of diffusing fluorine atoms

$$F + HCN \longrightarrow HFC=N^\bullet, \qquad (31)$$

while radical $FC^\bullet=NH$ is produced in the solid matrix as a result of photoinduced conversion of stabilised radical $HFC=N^\bullet$

$$HFC=N^\bullet \xrightarrow{h\nu} FC^\bullet=NH. \qquad (32)$$

Selective excitation to the absorption band of the $\tilde{X}\,^2A' \rightarrow \tilde{A}\,^2A''$ electronic transition of radical $HFC=N^\bullet$ causes a complete conversion of this species into the other structural isomer. The resolved EPR spectra of both structural isomers are shown in Fig. 15. Based on the results of kinetic measurements and analysis of the absorption and fluorescence spectra of

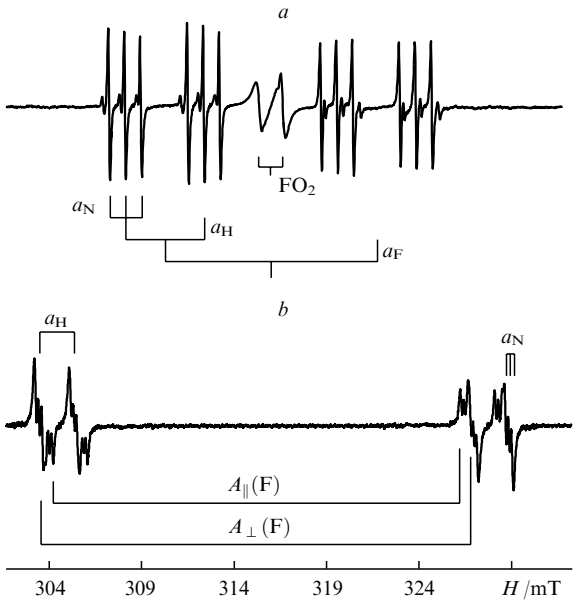


Figure 15. EPR spectra of $HFC=N^\bullet$ (*a*) and $FC^\bullet=NH$ (*b*) radicals stabilised in solid argon at 35 K.[169]
The radical was produced in the reactions of diffusing fluorine atoms with HCN molecules (*a*); the radical was generated by photolysis of trapped $HFC=N^\bullet$ radicals with light at $\lambda = 450 – 490$ nm (*b*). Shown are the HFS of the spectra of the radicals.

HFC=N$^{\bullet}$ and DFC=N$^{\bullet}$, it was concluded that irreversible reaction (32) is due to intramolecular tunnelling of hydrogen atoms on the PES of the electronically excited state.[169,170] The structure of these species was determined by comparing the calculated and experimental spectroscopic characteristics (a complete set of vibrational frequencies and IHFC constants).

VI. Chemical reactions involving oxygen atoms

Chemical reactions with participation of oxygen atoms in cryogenic matrices were mostly investigated in order to study the elementary processes initiated by photolysis of ozone molecules. In particular, it was found that the O_3 molecule is an efficient photolytic precursor for generation of oxygen atoms. In the text below we will consider the following aspects of these studies: the behaviour of photogenerated oxygen atoms in inert matrices, photochemical reactions in isolated molecular complexes [O_3–M] and chemical transformations initiated by photolysis of ozone in solid O_3 and O_2.

1. Oxygen atoms in solid matrices and crystals of inert gases

Photolytic generation of oxygen atoms in solid matrices has been studied in the course of photodissociation of isolated molecules O_3, O_2 and N_2O. In the gas phase excitation of O_3 molecules by light to the Hartley absorption band, $X^1A_1 \rightarrow 1\,^1B_2$, causes generation of a singlet oxygen atom with a quantum yield of 0.9

$$O_3 \xrightarrow{h\nu} O_2(^1\Delta_g) + O(^1D). \quad (33)$$

Another dissociation channel, with a quantum yield of 0.1,

$$O_3 \xrightarrow{h\nu} O_2(^3\Sigma_g) + O(^3P) \quad (34)$$

arises due to interception of the excited term $1\,^1B_2$ with the dissociative term that correlates with the ground state of the ozone molecule. UV-Photolysis of ozone in solid argon occurs with a low quantum yield ($\sim 10^{-1}$–10^{-3}) due to a strong cage effect.[171–173] The quantum yield of photolysis of ozone monomers in solid argon as a function of temperature is presented Figure 16. A dramatic weakening of the cage effect with an increase in temperature was rationalised by an increase in the amplitude of the O_3 librations at the lattice site.[171] The quantum yield of photolysis of ozone in solid xenon is close to unity. However, nearly 80% of the stabilised atoms recombine with the neighbouring oxygen molecules after warm-up to 30–40 K.[174] Other atoms react with distant dioxygen molecules or undergo bulk recombination. By analysing the kinetics of geminate recombination

$$O + O_2 \longrightarrow O_3,$$

it was concluded [174] that the thermalisation length of 'hot' oxygen atoms ($\sim$0.2 nm) is comparable with the binding distance between the diffusing atom and the dioxygen molecule. The weak influence of the cage effect on photodissociation of ozone was rationalised by the fact that the effective radius of the interaction Rg–O(^{1}D) is much smaller than that of the interaction Rg–O(^{3}P).[71,175] Therefore, ozone molecules are considered as convenient photolytic precursors for generation of reactive oxygen atoms, O(^{1}D), in low-temperature matrices.[173,176,177] For instance, the formation of N_2O in the photolysis of ozone molecules in solid nitrogen [177] is energetically possible only in the reaction of a singlet atom with an N_2 molecule

$$[O_3]_{N_2} \xrightarrow{h\nu} [O(^1D) + O_2]_{N_2} \longrightarrow N_2O\cdots O_2. \quad (34a)$$

Another channel of O_3 photolysis causes stabilisation of the O(^{3}P) atom outside the reaction cage

$$[O_3]_{N_2} \xrightarrow{h\nu} [O(^1D) + O_2]_{N_2} \longrightarrow [O_2]_{N_2} + O(^3P). \quad (34b)$$

The mass-balance equation for the reaction products showed [177] that the formation of one N_2O molecule in reaction (34a) 'costs' a total of fifteen dissociated O_3 molecules. The fact that the N_2O molecules are formed only in complexes with O_2 unequivocally indicates that reaction (34a) occurs with participation of the N_2 molecules surrounding the ozone molecule and that the oxygen atoms outside the parent cage do not react with distant nitrogen molecules. At the same time a value of 0.7 was reported [176] for the quantum yield of O_3 photodissociation in a solid nitrogen matrix at 10 K. Taking into account the results obtained by Schriver-Mazzuoli *et al.*,[177] this means that the main process is exit of the 'hot' atom from the cage followed by stabilisation of the O(^{3}P) atom [reaction (34b)]. If the atom does not escape the parent cage, either the O + O_2 recombination or 'concerted' reaction (34a) with participation of the oxygen atom and O_2 and N_2 molecules occur. Therefore, the efficiency of reaction (34a) should be compared with that of the competing reaction of inverse recombination to the cage. Comparison of the data reported in Refs 176 and 177 suggests that the ratio of yields of these reactions is $\sim$1 : 6.

In the example just considered the reaction involved the O(^{1}D) atom located within the parent cage. Chemical reactions of photogenerated atoms O(^{1}D) outside the cage were discovered in studies of photolysis of ternary mixtures Ar/O_3/hydrocarbon.[178,179] In particular, it was shown that the main channel of the reaction of the O(^{1}D) atom with methane and methanol molecules is insertion of this atom into the C–H bond, which causes stabilisation of the reactive intermediates:

$$O(^1D) + CH_4 \longrightarrow CH_3OH, \quad (35)$$
$$O(^1D) + CH_3OH \longrightarrow CH_2(OH)_2.$$

These results supported the effect of insertion of the oxygen atom into the C–H bond, which was reported earlier.[180,181] The results of recent studies of the O + CH_4 interaction in molecular beams and analysis of its dynamics in the framework of the Rice–Ramsperger–Kassel–Markus (RRKM) statistical theory showed that the end products (mostly $CH_3^{\bullet}$ + OH and CH_2O + H) are formed after dissociation of vibrationally excited intermediate (CH_3OH)* characterised by a lifetime of $\sim 10^{-11}$ s. Direct reaction of hydrogen abstraction contributes insignificantly to the balance of end products (see, *e.g.*, Ref. 182).

The problem of distinguishing the reaction channels associated with the oxygen atoms generated by photolysis of O_3 molecules consists in that the van der Waals complexes of ozone with other molecules are, as a rule, characterised by small frequency shifts in the IR spectra. Therefore, discrimination between the reaction products formed by photolysis of binary complexes [O_3–M] and the products of reactions of migrating 'hot' atoms with distant molecules is not necessarily successful. The best results were obtained in studies of ozone photolysis in charge-transfer complexes. A correlation was found between consumption of the photolysed [O_3···M] complexes and the formation of the products of photolysis. As a rule, such reactions are completed with transfer of oxygen atom from the photoexcited O_3 molecule to the partner in the complex

$$[O_3\cdots M] \xrightarrow{h\nu} [O_2 + OM]. \quad (36)$$

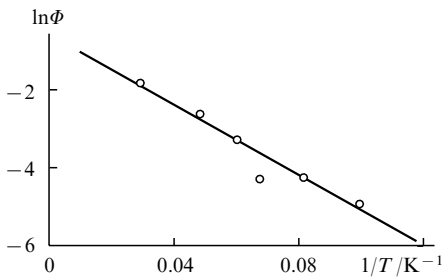


Figure 16. Quantum yield (Φ) of photolysis of ozone monomers in solid argon as a function of temperature.[171]

Table 8. Primary products of photoinitiated reactions in [O_3---M] complexes isolated in solid argon.

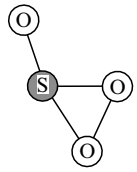
Complex	Photoinitiation wavelength range /nm	Product	Ref.
[O_3---H_2O]	266	H_2O_2	183
[O_3---Cl_2]	800 – 360	ClClO	184
[O_3---Br_2]	800 – 360	BrBrO	184
[O_3---BrCl]	800 – 360	ClBrO	184
[O_3---ICl]	750 – 470	ClIO	185
[O_3---CH_3I]	470 – 360	CH_3IO	186
[O_3---C_2H_5I]	< 800	C_2H_5IO	187
[O_3---CF_3I]	1000 – 470	CF_3IO	188
[O_3---PH_3]	633 – 515	H_3PO	189
[O_3---PCl_3]	1000 – 360	Cl_3PO	190
[O_3---PBr_3]	1000 – 360	Br_3PO	190
[O_3---P_4]	1000 – 590	P_4O	191
[O_3---AsH_3]	1000 – 630	H_3AsO	192
[O_3---SO_2]	266	SO_3	193
[O_3---H_2O_2]	266	H_2O_3	194

Table 8 lists the data on the products of photoinduced reactions (36). Reliable distinction between the reaction channels was reported recently [193] in a study of photolytic reactions of O_3 with SO_2 molecules. Using spectral and kinetic methods, they distinguished between the reactions of photogenerated $O(^1D)$ atoms with distant SO_2 molecules and transformations in the photolysed complexes [O_3---SO_2]. The only product detected was a symmetric oxide SO_3. Besides, experiments with the $^{16}O \rightarrow {}^{18}O$ isotope substitution revealed an efficient exchange of oxygen atoms between the reactants

$$^{18}O + {}^{16}OS^{16}O \longrightarrow [OSO_2]^* \longrightarrow {}^{16}O + {}^{16}OS^{18}O, \quad (37a)$$

$$[{}^{16}OS^{16}O + {}^{18}O_3] \xrightarrow{h\nu} [{}^{16}OS^{18}O + {}^{16}O^{18}O^{18}O]. \quad (37b)$$

Taking into account the results obtained, the authors suggested the existence of vibrationally excited asymmetric isomer $(OSO_2)^*$ as reactive intermediate.



Among five structural isomers of SO_3 predicted by quantum-chemical calculations,[61] the above-mentioned isomer is less stable than symmetric SO_3 (the energy difference is 230 kJ mol^{-1}). The conclusion [193] that the excited intermediate does not correspond to the symmetric structure of the most stable isomer (D_{3h} symmetry) was based on the assumption that the isotope composition of the products of reactions (37a) and (37b) does not correspond to the structure of the $(SO_3)^*$ intermediate containing three equivalent oxygen atoms.

At present, the available experimental data on the mobility of thermalised oxygen atoms in the solid cryogenic matrices and crystals are inadequate to correctly describe diffusion of such atoms even phenomenologically. The kinetics of thermally induced loss of oxygen atoms in a solid xenon matrix in the temperature range 30 – 40 K [69, 195, 196] was described by two rate constants corresponding to the diffusion coefficients of 1.4×10^{-15} and 5.4×10^{-18} cm^2 s^{-1} at 32 K. Thermal diffusion of oxygen atoms in the crystals of krypton and xenon was also studied.[68] The loss of the O atoms was described by three activation barriers assuming the existence of three types of atomic sites in the crystal lattice. Calculations of the mobility of oxygen atoms in a xenon crystal, carried out in the framework of the transition state theory using various types of pair potentials for the interaction of the $O(^3P)$ atom with the atoms of the crystal, gave somewhat contradictory results. For instance, the diffusion coefficients reported by Guo and Thompson [197] are three to five orders of magnitude higher than those calculated by Ford *et al.*,[198] whereas the corresponding experimental values [68, 69] lie between them. These discrepancies can be understood if we take into account the fact that the barriers to diffusion are determined by the short-range terms of the pair interaction potentials and that thermally activated processes occurring at ultralow temperature are very sensitive to the height of the activation barrier. In addition, differences in morphology between the matrices and crystalline samples predetermine a wide scatter of the activation barriers.

Another phenomenological model of thermally activated mobility of atomic oxygen was proposed by Danilychev and Apkaryan [68, 71] who postulated that the oxygen atom in the ground state, $O(^3P)$, in the crystal is immobile. It was also assumed that thermally induced intersystem crossing $O(^3P) \rightarrow O(^1D)$, which occurs with participation of the lattice phonons, is followed by migration of the atom across the singlet PES $O(^1D) - (Xe)_n$ until recrossing and stabilisation in the crystal. According to calculations,[71] $O - (Xe)_n$ intersystem crossing is possible in crystalline xenon. Bringing forward arguments in support of this diffusion mechanism, it was emphasised that the length of thermally activated migration appears to be comparable with the migration length of the $O(^1D)$ atoms generated by photoexcitation of stabilised atoms. Nevertheless, the possibility for this diffusion mechanism to occur is still a moot question (see review [10]). The multiplicity of diffusing atoms can be experimentally determined by following their reactions with impurity molecules, which proceed involving the singlet atoms only. Earlier, such reactions were observed for 'hot' $O(^1D)$ atoms generated in the photodissociation of ozone molecules in solid argon (see, *e.g.*, Refs 173 and 178).

2. Chemical transformations initiated by photolysis of ozone in solid oxygen and ozone matrices

Photodecomposition of ozone upon UV photolysis to the Hartley absorption band in the gas phase occurs with a quantum yield of ~ 4.[199] Both products of primary photodissociation [see Eqn (33)] participate in further reactions to give a total of six oxygen molecules

$$O(^1D) + O_3 \longrightarrow 2O_2, \quad (38)$$

$$O_2(^1\Delta_g) + O_3 \longrightarrow O(^3P) + 2O_2, \quad (39)$$

$$O(^3P) + O_3 \longrightarrow 2O_2. \quad (40)$$

Photolysis of thin films of pure ozone at 10 K occurs with a quantum yield of 2.0 ± 0.3 (see Ref. 171). This means that photodecomposition of ozone in the solid phase involves two successive stages, namely, photodissociation (33) characterised by a quantum yield close to unity and the reaction of one photodecomposition product with the O_3 molecule. Among the three feasible secondary reactions (38) – (40), reaction (38) with participation of the $O(^1D)$ atom seems to be the most probable,[171] since the activation barriers to the other two reactions in the gas phase are rather high (> 15 kJ mol^{-1}). Analogous transformations were found in the case of UV photolysis of ozone dimers isolated in solid argon [171]

$$[O_3\text{---}O_3] \xrightarrow{h\nu} [O_2 + O(^1D) + O_3] \longrightarrow [O_2 + O_2 + O_2]. \quad (41)$$

The results obtained by Schriver-Mazzuoli *et al.*[200] supported high efficiency of photolysis of the [O_3---O_3] dimers in solid argon. However, based on the kinetic data, they proposed another mechanism of loss of the dimers which leads to stabilisation of the oxygen atom

$$[O_3\text{---}O_3] \xrightarrow{h\nu} [O_2 + O_4^*] \longrightarrow O_2 + O + O_3. \quad (42)$$

The main difficulty distinguishing between the reaction channels (41) and (42) is that only consumption of the ozone molecules was studied by IR spectroscopy.[171,200] In this case kinetic measurements cannot provide a means for reliable determination of the product ratios for reactions (41) and (42). The results of IR spectroscopic investigations can be essentially supplemented by carrying out experiments with isotope substitution in the molecules of initial reactants. For instance, photolysis of ozone molecules in solid oxygen was studied using the isotope substitution of oxygen atoms.[201] The main idea of this experimental strategy was to trap the ^{18}O-enriched ozone molecules in the solid oxygen matrix containing the ^{16}O atoms only. Figure 17 illustrates the evolution of the IR spectrum of ozone in the region of the ν_3 vibration during continuous photolysis with light at a wavelength of 693 nm to the Chappuis absorption band. Changes in the spectrum show that the number of the O_3 molecules remains constant during long-term irradiation. However, the isotope composition of ozone molecules changes radically, namely, the $^{18}O_3$(18-18-18) molecules are replaced by the $^{16}O_3$(16-16-16) molecules during photolysis. Kinetic analysis showed that the atom produced upon photodissociation of O_3 is added to the neighbouring O_2 molecule to give an O_3 molecule with altered isotope composition. Subsequent photolysis of products of these reactions causes further transfer of the ^{18}O atoms in the O_2 molecules and, correspondingly, enrichment of the ozone molecules with the ^{16}O isotope

$$O_3(16\text{-}16\text{-}18) \xrightarrow{h\nu} O_2(16\text{-}16) + O(18), \quad (43a)$$

$$O_3(16\text{-}16\text{-}18) \xrightarrow{h\nu} O_2(16\text{-}18) + O(16), \quad (43b)$$

$$O_3(16\text{-}18\text{-}16) \xrightarrow{h\nu} O_2(16\text{-}18) + O(16), \quad (43c)$$

$$O(16) + O_2(16\text{-}16) \longrightarrow O_3(16\text{-}16\text{-}16). \quad (43d)$$

In fact this reaction mechanism describes a photoinduced chemical migration of ozone molecules in solid oxygen. The use of isotope substitution allowed reliable establishment of reaction channels in the case where the reactants and products are comprised of oxygen atoms only.[201]

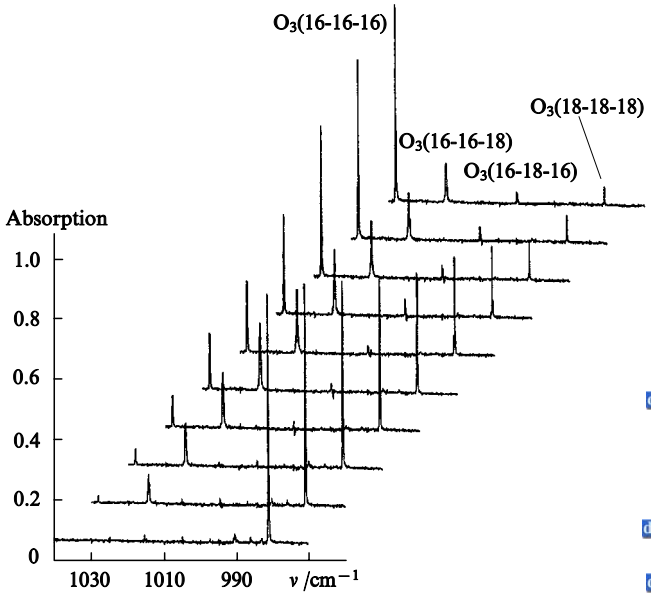


Figure 17. Evolution of the IR spectrum of ozone in the region of the ν_3 vibration during continuous photolysis of a $^{18}O_3 : {}^{16}O_2 = 1 : 4000$ sample with light ($\lambda = 693$ nm).[201]

VII. Conclusion

The results of experimental and theoretical investigations considered in this review show that chemical reactions of mobile atoms, which occur in an inert crystalline environment at ultralow temperature, cause stabilisation of free radicals and radical–molecular complexes (short-lived intermediate particles in the gas phase). The use of mobile atoms for generation of reactive intermediates permitted obtaining spectroscopic data on new metastable molecular structures which were not observed by other methods. This type of reaction is characterised by a rather high extent of conversion of the initial reactants, which makes it possible to detect matrix-isolated products of primary reactions. Stabilisation of a particular type of isolated particles is due to high selectivity of cryochemical reactions. This permits detection of matrix-isolated products of primary reactions using conventional methods of low-temperature spectroscopy. Joint use of the IR, optical and EPR spectroscopy allows reliable identification of products and establishment of their structure by comparing the measured spectroscopic characteristics with the results of quantum-chemical calculations.

The use of mobile atoms for cryochemical synthesis of new compounds is not limited to the atoms of three elements and their reactions considered in this review. In particular, of considerable interest is the use of photostimulated mobility of the rare-earth metal atoms and transition metal atoms. The results of such studies carried out before 1999 were generalised in a monograph.[202] Experimental approaches to low-temperature synthesis of particles containing various metal atoms and clusters have been reviewed.[203]

The fact that international conferences on the chemistry and physics of matrix-isolated species and on low-temperature chemistry are held on a regular basis (in particular, the last two conferences were held in Poland [204] and Finland [205]) points out that this review is topical. When preparing the manuscript, the authors of this review used not only original communications but also information obtained in discussions, which is useful for refinement of researchers' views of particular (including moot) questions.

This review has been written with financial support from the Russian Foundation for Basic Research (Project No. 01-03-33171).

References

1. A H Zewail *J. Phys. Chem. A* **104** 5660 (2000)
2. O M Sarkisov, S Ya Umanskii *Usp. Khim.* **70** 515 (2001) [*Russ. Chem. Rev.* **70** 449 (2001)]
3. E Whitle, D A Dows, G C Pimentel *J. Chem. Phys.* **22** 1943 (1954)
4. I Norman, G Porter *Nature (London)* **174** 508 (1954)
5. M E Jacox *J. Phys. Chem. Ref. Data* **27** 115 (1998)
6. M E Jacox *Rev. Chem. Intermed.* **2** 1 (1978)
7. L Andrews, M Moskovits (Eds) *Chemistry and Physics of Matrix-Isolated Species* (Amsterdam: Elsevier, 1989)
8. V E Bondybey, A M Smith, J Agreiter *Chem. Rev.* **96** 2113 (1996)
9. D E Milligan, M E Jacox *J. Chem. Phys.* **38** 2627 (1963)
10. V A Apkarian, N Schwentner *Chem. Rev.* **99** 1481 (1999)
11. M Moskovits, G Ozin (Eds) *Cryochemistry* (New York: Wiley, 1976)
12. G B Sergeev, V A Batyuk *Kriokhimiya* (Cryochemistry) (Moscow: Khimiya, 1978)
13. M E Jacox *Chem. Phys.* **189** 149 (1994)
14. Y Haas, U Samuni *Prog. React. Kinet. Mech.* **23** 211 (1998)
15. Z Bihary, R B Gerber, V A Apkarian *J. Chem. Phys.* **115** 2695 (2001)
16. E F C Byrd, C D Sherrill, M Head-Gordon *J. Phys. Chem. A* **105** 9736 (2001)
17. L Abouaf-Marguin, M E Jacox, D E Milligan *J. Mol. Spectrosc.* **67** 34 (1977)
18. A Heikkila1, J Lundell *J. Phys. Chem. A* **104** 6637 (2000)

19. P Beichert, D Pfeiler, E Knözinger *Ber. Bunsen-Ges. Phys. Chem.* **99** 1469 (1995)
20. E Ya Misochko, A V Akimov, C A Wight *Chem. Phys. Lett.* **274** 23 (1997)
21. E Ya Misochko, A V Akimov, C A Wight *Chem. Phys. Lett.* **293** 547 (1998)
22. I U Goldschleger, A V Akimov, E Ya Misochko, C A Wight *J. Mol. Spectrosc.* **205** 269 (2001)
23. M E Jacox *Chem. Phys.* **53** 307 (1980)
24. M Shiotani, Y Nagata, J Sohma *J. Phys. Chem.* **86** 4131 (1982)
25. E Ya Misochko, V A Benderskii, A U Goldschleger, A V Akimov, A V Benderskii, C A Wight *J. Chem. Phys.* **106** 3146 (1997)
26. R W Fessendern, R H Schuler *J. Chem. Phys.* **39** 2147 (1963)
27. S Ya Pshezhetskii, A G Kotov, V K Milinchuk, V A Roginskii, V I Tupikov, in *EPR Svobodnykh Radikalov v Radiatsionnoi Khimii* (EPR of Free Radicals in Radiation Chemistry) (Moscow: Khimiya, 1972) p. 140
28. T Kumada, J Kumagai, T Miyazaki *J. Chem. Phys.* **114** 10 024 (2001)
29. C A McDowell, P Raghunathan, K Shimokoshi *J. Chem. Phys.* **58** 114 (1973)
30. R W Fessenden *J. Chem. Phys.* **37** 747 (1962)
31. T Miyazaki, K Yamamoto, J Arai *Chem. Phys. Lett.* **219** 405 (1994)
32. E L Cochran, F J Adrian, V A Bowers *J. Chem. Phys.* **34** 1161 (1961)
33. K Toriyama, M Iwasaki, K Nunome, H Muto *J. Chem. Phys.* **75** 1633 (1981)
34. E L Cochran, F J Adrian, V A Bowers *J. Phys. Chem.* **74** 2083 (1970)
35. F J Adrian *J. Chem. Phys.* **46** 1543 (1967)
36. E L Cochran, F J Adrian, V A Bowers *J. Chem. Phys.* **44** 4626 (1966)
37. A V Akimov, Candidate Thesis in Physical and Mathematical Sciences, Institute of Problems of Chemical Physics, Russian Academy of Sciences, Chernogolovka, 2001
38. W Weltner Jr *Magnetic Atoms and Molecules* (Mineola, NY: Dover, 1989)
39. L B Knight, D J Tyler, P Kudelko, J B Lyon, A J McKinley *J. Chem. Phys.* **99** 7384 (1993)
40. A U Goldschleger, Candidate Thesis in Physical and Mathematical Sciences, State Scientific Center of Russian Federation 'L Ya Karpov Institute of Physical Chemistry', Moscow, 1997
41. Y Chen, A Rauk, E Tschuikov-Roux *J. Chem. Phys.* **93** 6620 (1990)
42. K S Chen, P J Krusic, P Meakin, J K Kochi *J. Phys. Chem.* **78** 2014 (1974)
43. V Barone, C Adamo, N Russo *Chem. Phys. Lett.* **212** 5 (1993)
44. V Barone *Theor. Chim. Acta* **91** 113 (1995)
45. V Barone, in *Recent Advances in Density Functional Methods* Pt. I (Ed. D P Chong) (Singapore: World Scientific, 1995) p. 287
46. I U Goldschleger, A V Akimov, E Ya Misochko *J. Mol. Struct.* **519** 191 (2000)
47. E Y Misochko, I U Goldschleger, A V Akimov, C A Wight *Low Temp. Phys.* **26** 727 (2000)
48. V E Bondybey, L E Brus *Adv. Chem. Phys.* **41** 269 (1980)
49. J Goodman, L E Brus *J. Chem. Phys.* **67** 4858 (1977)
50. V E Bondybey, A Nitzan *Phys. Rev. Lett.* **38** 889 (1977)
51. A Toma, G Schallmoser, A M Smith, B E Wurfel, V E Bondybey *J. Chem. Phys.* **100** 5387 (1994)
52. K Johnsson, A Engdahl, P Ouis, B Nelander *J. Phys. Chem.* **97** 9603 (1993)
53. H S P Muller, H Willner *J. Phys. Chem.* **97** 10 589 (1993)
54. L H Lai, C P Liu, Y P Lee *J. Chem. Phys.* **109** 968 (1998)
55. H Frei, G C Pimentel, in *Chemistry and Physics of Matrix-Isolated Species* (Eds L Andrews, M Moskovits) (Amsterdam: Elsevier, 1989) p. 139
56. L M Raff, in *Modern Methods for Multidimensional Dynamics Computations in Chemistry* (Ed. D L Thompson) (Singapore: World Scientific, 1998) p. 266
57. K Johnsson, A Engdahl, P Ouis, B Nelander *J. Mol. Struct.* **293** 137 (1993)
58. L Andrews *J. Phys. Chem.* **88** 2940 (1984)
59. K C Klemitshaw, J R Sodeau *J. Phys. Chem.* **93** 3552 (1989)
60. A V Akimov, I U Goldschleger, E Ya Misochko, C A Wight *J. Phys. Chem. A* **42** 9756 (2002)
61. S H Jou, M Y Shen, C H Yu, Y P Lee *J. Chem. Phys.* **104** 5745 (1996)
62. C L Lee, Y P Lee, X F Wang, Q Z Qin *J. Chem. Phys.* **109** 10446 (1998)
63. N Schwentner, V A Apkarian *Chem. Phys. Lett.* **154** 413 (1989)
64. A I Katz, J Feld, V A Apkarian *Opt. Lett.* **14** 441 (1989)
65. H Kunttu, J Feld, R Alimi, A Becker, V A Apkarian *J. Chem. Phys.* **92** 4856 (1990)
66. J Feld, H Kunttu, V A Apkarian *J. Chem. Phys.* **93** 1009 (1990)
67. W G Lawrence, V A Apkarian *J. Chem. Phys.* **97** 6199 (1992)
68. A Danilychev, V A Apkarian *J. Chem. Phys.* **99** 8617 (1993)
69. E T Ryan, E Weitz *J. Chem. Phys.* **99** 8628 (1993)
70. K Kizer, V A Apkarian *J. Chem. Phys.* **103** 4945 (1995)
71. A Danilychev, V A Apkarian *J. Chem. Phys.* **100** 5556 (1994)
72. R Alimi, R B Gerber, V A Apkarian *J. Chem. Phys.* **92** 3551 (1990)
73. R Schriever, M Chergui, H Kunz, K V Stepanenko, N Schwentner *J. Chem. Phys.* **91** 4128 (1989)
74. E L Cochran, V A Bowers, S N Forner, C K Jen *Phys. Rev. Lett.* **2** 43 (1959)
75. F J Adrian *J. Chem. Phys.* **32** 972 (1960)
76. T Miyazaki, A Wakahara, T Usui, K Fueki *J. Chem. Phys.* **86** 3881 (1982)
77. H H Grunberg, H Gabriel *Chem. Phys. Lett.* **192** 503 (1992)
78. J Eloranta, K Vaskonen, H Kunttu *J. Chem. Phys.* **110** 7917 (1999)
79. D LaBrake, E T Ryan, E Weitz *J. Chem. Phys.* **102** 4112 (1995)
80. D LaBrake, E Weitz *Chem. Phys. Lett.* **221** 430 (1993)
81. V I Feldman, F F Shukhov *Chem. Phys. Lett.* **255** 425 (1996)
82. J Eberlein, M Greuzburg *J. Chem. Phys.* **106** 2188 (1997)
83. V I Feldman, F F Sukhov, A Ya Orlov *Chem. Phys. Lett.* **280** 507 (1997)
84. K Vaskonen, J Eloranta, T Kiljunen, H Kunttu *J. Chem. Phys.* **110** 2122 (1999)
85. E B Gordon, A A Pel'menev, O F Pugachev, V V Khmelenko *Pis'ma Zh. Esp. Teor. Fiz.* **37** 237 (1983) [a]
86. L V Ivliev, A S Isakovskikh, A Ya Katunin, I I Lukashevich, V V Sklyarevskii, V V Suraev, V V Filippov, N I Filippov, V A Shevtsov *Pis'ma Zh. Esp. Teor. Fiz.* **38** 317 (1983) [a]
87. H Tsuruta, T Miyazaki, N Azuma *J. Phys. Chem.* **87** 5422 (1983)
88. K Komaguchi, T Kumada, Y Aratono, T Miyazaki *Chem. Phys. Lett.* **268** 493 (1997)
89. K Komaguchi, T Kumada, T Takayanagi, Y Aratono, M Shiotani, T Miyazaki *Chem. Phys. Lett.* **300** 257 (1999)
90. T Miyazaki, H Morikita, K Fueki, T Hiraku *Chem. Phys. Lett.* **182** 35 (1991)
91. R Hoppe, W Dahne, H Mattauch, K H Rodder *Angew. Chem.* **74** 903 (1962)
92. H H Claassen, H Selig, J G Malm *J. Am. Chem. Soc.* **84** 3593 (1962)
93. J G Malm, H Selig, J Jortner, S A Rice *Chem. Rev.* **65** 199 (1965)
94. K Seppelt, D Lentz *Prog. Inorg. Chem.* **29** 167 (1982)
95. J H Holloway, E G Hope *Adv. Inorg. Chem.* **46** 51 (1999)
96. G Frenking, D Cremer, in *Structure and Bonding, Noble Gas and High Temperature Chemistry* (Eds M J Clarke, J B Goodenough, J A Ibers, C K Jorgensen, D M P Mingos, J B Neilands, G A Palmer, D Reinen, P J Sadler, R Weiss, R J P Williams) (Berlin: Springer, 1990) p. 17
97. L Y Nelson, G C Pimentel *Inorg. Chem.* **6** 1758 (1967)
98. J J Turner, G C Pimentel *Science* **140** 975 (1963)
99. W F Howard, L Andrews *J. Am. Chem. Soc.* **96** 7864 (1974)
100. M Pettersson, J Lundell, M Rasanen *J. Chem. Phys.* **102** 6423 (1995)
101. M Pettersson, J Lundell, M Rasanen *J. Chem. Phys.* **103** 205 (1995)
102. M Pettersson, J Nieminen, L Khriachtchev, M Rasanen *J. Chem. Phys.* **107** 8423 (1997)
103. M Pettersson, J Lundell, M Rasanen *Eur. J. Inorg. Chem.* 729 (1999)

104. J Lundell, L Khriachtchev, M Pettersson, M Rasanen *Low Temp. Phys.* **26** 680 (2002)
105. I Last, T F George *J. Chem. Phys.* **89** 3071 (1988)
106. J Ahokas, K Vaskonen, J Eloranta, H Kunttu *J. Phys. Chem. A* **104** 9506 (2000)
107. L Khriachtchev, H Tanskanen, M Pettersson, M Rasanen, J Ahokas, H Kunttu, V Feldman *J. Chem. Phys.* **116** 5649 (2002)
108. M Lorenz, M Rasanen, V E Bondybey *J. Phys. Chem. A* **104** 3770 (2000)
109. L Khriachtchev, H Tanskanen, M Pettersson, M Rasanen, V Feldman, F Shukhov, A Orlov, A Shestakov *J. Chem. Phys.* **116** 5708 (2002)
110. L Khriachtchev, M Pettersson, N Runeberg, J Lundell, M Rasanen *Nature (London)* **406** 874 (2000)
111. N Runeberg, M Pettersson, L Khriachtchev, J Lundell, M Rasanen *J. Chem. Phys.* **114** 836 (2001)
112. R E Boltnev, E B Gordon, I N Krushinskaya, A A Pel'menev, E A Popov, O F Pugachev, V V Khmelenko *Fiz. Nizkikh Temp.* **18** 819 (1992)
113. E B Gordon, V V Khmelenko, A A Pelmenev, E A Popov, O F Pugachev, A F Shestakov *Chem. Phys.* **170** 411 (1993)
114. R E Boltnev, E B Gordon, I N Krushinskaya, A A Pelmenev, D Yu Stolyarov, V V Khmelenko *Chem. Phys. Lett.* **305** 217 (1999)
115. W E Jones, G Skolnik *Chem. Rev.* **76** 563 (1976)
116. V N Kondrat'ev *Konstanty Skorosti Gazofaznykh Reaktsii* (Rate Constants of Gas-Phase Reactions) (Moscow: Nauka, 1970)
117. M E Jacox, in *Chemistry and Physics of Matrix-Isolated Species* (Eds L Andrews, M Moskovits) (Amsterdam: Elsevier, 1989) p. 75
118. V E Bondybey, C Fletcher *J. Chem. Phys.* **64** 3615 (1976)
119. V E Bondybey, L E Brus *J. Chem. Phys.* **64** 3724 (1976)
120. M Mandich, P Beeken, G Flynn *J. Chem. Phys.* **77** 702 (1982)
121. C Bressler, M Dickgiesser, N Schwentner *J. Chem. Phys.* **107** 10 268 (1997)
122. A Arkell *J. Am. Chem. Soc.* **87** 4057 (1965)
123. R D Spratley, J J Turner, G C Pimentel *J. Chem. Phys.* **44** 2063 (1966)
124. G L Johnson, L Andrews *J. Am. Chem. Soc.* **102** 5736 (1980)
125. R D Hunt, L Andrews *Inorg. Chem.* **26** 3051 (1987)
126. E Ya Misochko, V A Benderskii, A U Goldschleger, A V Akimov, A V Benderskii, Ch A Uait *Izv. Akad. Nauk, Ser. Khim.* 718 (1997) [b]
127. J M Parson, Y T Lee *J. Chem. Phys.* **56** 4658 (1972)
128. V A Benderskii, A U Goldschleger, A V Akimov, E Ya Misochko, C A Wight *Mendeleev Commun.* **5** 245 (1995)
129. E Ya Misochko, A V Benderskii, C A Wight *J. Phys. Chem.* **100** 4496 (1996)
130. L P Davis, L W Burggraf, M S Gordon, K K Baldrige *J. Am. Chem. Soc.* **107** 4415 (1985)
131. J C Corchado, J Espinosa-Garcia *J. Chem. Phys.* **105** 3152 (1996)
132. M E Jacox *J. Chem. Phys.* **83** 3255 (1985)
133. I U Goldschleger, Candidate Thesis in Physical and Mathematical Sciences, Institute of Problems of Chemical Physics, Russian Academy of Sciences, Chernogolovka, 2001
134. M E Jacox *Chem. Phys.* **59** 199 (1981)
135. M E Jacox *Chem. Phys.* **42** 133 (1979)
136. L Andrews, G L Johnson *J. Phys. Chem.* **88** 425 (1984)
137. G L Johnson, L Andrews *J. Am. Chem. Soc.* **105** 163 (1983)
138. G L Johnson, L Andrews *J. Am. Chem. Soc.* **104** 3043 (1982)
139. D M Neumark, A M Wodtke, G N Robinson, C C Hayden, K Shobotake, R K Sparks, T P Schafer, Y T Lee *J. Chem. Phys.* **82** 3067 (1985)
140. W B Chapman, B W Blacmon, D J Nesbitt *J. Chem. Phys.* **107** 8193 (1997)
141. V M Azriel, L Yu Rusin, M B Sevryuk, J P Toennnies *Chem. Phys.* **232** 307 (1998)
142. K Stark, H J Werner *J. Chem. Phys.* **104** 6515 (1996)
143. A U Goldschleger, E Ya Misochko, A V Akimov, I U Goldschleger, V A Benderskii *Chem. Phys. Lett.* **267** 288 (1997)
144. D J Donaldson, J J Sloan, J D Goddard *J. Chem. Phys.* **82** 4524 (1985)
145. S Wategaonkar, D W Sester *J. Chem. Phys.* **86** 4477 (1987)
146. D Goddard, D J Donaldson, J J Sloan *Chem. Phys.* **114** 321 (1987)
147. E Ya Misochko, I U Goldschleger, A V Akimov *Izv. Akad. Nauk, Ser. Khim.* 832 (2000) [b]
148. W B Fox, B Sukornick, J S Mackenzie, R L Sturtevant, A F Maxwell, J R Holmes *J. Am. Chem. Soc.* **92** 5240 (1970)
149. R R Smardzewski, W B Fox *J. Chem. Phys.* **60** 2193 (1974)
150. V B Rozenshtein, Yu R Bedzhanyan, S Ya Umanskii, Yu M Gershenzon *Khim. Fiz.* **6** 1659 (1987) [c]
151. K Nishikida, F Williams *J. Am. Chem. Soc.* **97** 7168 (1975)
152. E Ya Misochko, A V Akimov, I U Goldschleger, C A Wight *J. Am. Chem. Soc.* **120** 11 520 (1998)
153. E Ya Misochko, A V Akimov, I U Goldschleger, A I Boldyrev, C A Wight *J. Am. Chem. Soc.* **121** 405 (1999)
154. S S Prasad, W M Adams *J. Photochem.* **13** 234 (1980)
155. W M Adams *Nature (London)* **285** 152 (1980)
156. A Rauk, E Tschuikov-Roux, Y Chen, M P McGrath, L Radom *J. Phys. Chem.* **97** 7947 (1993)
157. E Ya Misochko, A V Akimov, C A Wight *J. Phys. Chem. A* **103** 7972 (1999)
158. R A Bair, T H Dunning Jr *J. Chem. Phys.* **82** 2280 (1985)
159. H Dupin, I Baraille, C Larrieu, A Dargelos *Chem. Phys.* **256** 7 (2000)
160. F Bernardi, F Cacace, G Occhiucci, A Ricci, I Rossi *J. Phys. Chem. A* **104** 5545 (2000)
161. P H Kasai, L A Eriksson *Mol. Phys.* **96** 993 (1999)
162. M E Jacox, D E Milligan *J. Chem. Phys.* **48** 4040 (1968)
163. M E Jacox *J. Phys. Chem.* **91** 6595 (1987)
164. S Yamamoto, S Saito *J. Chem. Phys.* **96** 4157 (1992)
165. R N Dixon, G Duxbury, R C Mitchell, J P Simons *Proc. R. Soc. London, Ser. A* **300** 405 (1967)
166. M Petterson, J Lundell, L Khriachtchev, M Rasanen *J. Chem. Phys.* **109** 618 (1998)
167. I U Goldschleger, A V Akimov, E Ya Misochko, C A Wight *Mendeleev Commun.* **11** 64 (2001)
168. E Ya Misochko, I U Goldschleger, A V Akimov, C A Wight *J. Am. Chem. Soc.* **123** 5156 (2001)
169. E Ya Misochko, A V Akimov, I U Goldschleger, C A Wight *J. Chem. Phys.* **116** 10318 (2002)
170. E Ya Misochko, A V Akimov, I U Goldschleger, C A Wight *J. Chem. Phys.* **116** 10307 (2002)
171. A V Benderskii, C A Wight *J. Chem. Phys.* **101** 292 (1994)
172. M Bahou, L Schriver-Mazzuoli, A Schriver *J. Chem. Phys.* **110** 8636 (1999)
173. X J Ning, L N Zhang, M H Chen, Q Z Qin *J. Chem. Phys.* **112** 386 (2000)
174. A V Benderskii, C A Wight *J. Chem. Phys.* **104** 85 (1996)
175. T H Dunning Jr, P J Hay *J. Chem. Phys.* **66** 3767 (1977)
176. A V Benderskii, C A Wight *Chem. Phys.* **189** 307 (1994)
177. M Bahou, L Schriver-Mazzuoli, C Camy-Peyret, A Schriver, T Chiavassa, J P Aycard *Chem. Phys. Lett.* **265** 145 (1997)
178. C Lugez, R Levant, A Schriver, L Schriver-Mazzuoli *Chem. Phys.* **181** 129 (1994)
179. M V Petterson, L Schriver-Mazzuoli, A Schriver, P Chaquin, E Lasson *Chem. Phys.* **204** 115 (1996)
180. W B DeMore, O F Raper *J. Chem. Phys.* **46** 2500 (1967)
181. R Withnall, L Andrews *J. Phys. Chem.* **92** 594 (1988)
182. C C Miller, R D van Zee, J C Stephenson *J. Chem. Phys.* **114** 1214 (2001)
183. L Schriver-Mazzuoli, C Barreau, A Schriver *Chem. Phys.* **140** 429 (1990)
184. L Schriver-Mazzuoli, A Schriver, P Chaquin *Chem. Phys.* **216** 105 (1997)
185. M Hawkins, L Andrews, A J Downs, D J Dury *J. Am. Chem. Soc.* **106** 3076 (1984)
186. M Hawkins, L Andrews *Inorg. Chem.* **24** 3285 (1985)
187. R J H Clark, J R Dann *J. Phys. Chem.* **100** 532 (1996)
188. L Andrews, M Hawkins, R Withnall *Inorg. Chem.* **24** 4234 (1985)
189. R Withnall, L Andrews *J. Phys. Chem.* **91** 784 (1987)
190. B W Moores, L Andrews *J. Phys. Chem.* **93** 1902 (1987)
191. L Andrews, R Withnall *J. Am. Chem. Soc.* **110** 5605 (1988)

192. L Andrews, R Withnall, B W Moores *J. Phys. Chem.* **93** 1279 (1987)
193. H Chaabouni, L Schriver-Mazzuoli, A Schriver *J. Phys. Chem. A* **104** 3498 (2000)
194. A Engdahl, B Nelander *Science* **295** 482 (2002)
195. H Krueger, E Weitz *J. Chem. Phys.* **96** 2846 (1992)
196. E T Ryan, E Weitz *J. Chem. Phys.* **99** 1004 (1993)
197. Y Guo, D L Thompson *J. Chem. Phys.* **103** 9024 (1995)
198. M B Ford, A D Foxworthy, G J Mains, L M Raff *J. Phys. Chem.* **97** 12134 (1993)
199. M P Popovich *Vestn. Mosk. Univ., Ser. 2, Khim.* **24** 219 (1983) [d]
200. M Bahou, L Schriver-Mazzuoli, A Schriver *J. Chem. Phys.* **114** 4045 (2001)
201. M Bahou, L Schriver-Mazzuoli, C Camy-Peyret, A Schriver *Chem. Phys. Lett.* **273** 31 (1997)
202. A D Pomogailo, A S Rozenberg, I E Uflyand *Nanochastitsy Metallov v Polimerakh* (Nanoparticles of Metals in Polymers) (Moscow: Khimiya, 2000)
203. G B Sergeev *Usp. Khim.* **70** 915 (2001) [*Russ. Chem. Rev.* **70** 809 (2001)]
204. *Proceedings of the Euroconference 2001 'The Chemistry and Physics of Matrix Isolated Species', Szklarska Poreba, Poland, 2001*
205. *Proceedings of the 4th International Conference on Low Temperature Chemistry, Jyväskylä, Finland, 2002*

[a] — *J. Exp. Theor. Phys. Lett. (Engl. Transl.)*
[b] — *Russ. Chem. Bull., Int. Ed. (Engl. Transl.)*
[c] — *Chem. Phys. Rep. (Engl. Transl.)*
[d] — *Moscow Univ. Bull. (Engl. Transl.)*